Did Galaxy Assembly and Supermassive Black-Hole Growth go Hand in Hand?

or: "Who came first: the Beauty or the Beast?

Rogier A. Windhorst (ASU)

Collaborators: Amber Straughn, Seth Cohen, Russell Ryan Jr., Nimish Hathi, Rolf Jansen, Sangeeta Malhotra, James Rhoads (ASU)

A. Koekemoer, N. Pirzkal, C. Xu, B. Mobasher, L. Strolger (STScI)

and Haojing Yan (SSC, Caltech)

Sponsored by NASA & STScI

hubblesite.org/newscenter/archive/2004/28/ *hubblesite.org/newscenter/archive/2006/04/*

Colloquium at UC Riverside, Thursday Apr. 12, 2007

"For God's sake, Edwards. Put the laser pointer away."

The danger of having Quasar-like devices too close to home ...

Outline

- (0) Introduction: Active Galactic Nuclei across the EM spectrum
- (1) Scientific Background and Goals:
- (1.a) Can we quantitatively establish if/how SMBH growth went hand-in-hand with galaxy assembly?
- (1.b) Was the epoch dependent rate of (minor) mergers the major driver of SMBH growth, AGN activity, and also of galaxy assembly?
- (2) Tadpole Galaxies in the HUDF: A measure of Galaxy Assembly?
- (3) A Study of Variable Objects in the HUDF: A measure of AGN Growth?
- (4) Summary and Conclusions
- (5) Future studies with James Webb and Hubble Wide Field Camera 3.

Sponsored by NASA

ASU Arizona State University

(0) The Cosmic Expansion and Contents of the Universe

Expansion $\Rightarrow$ redshift	$\lambda_{obs} = \lambda_{rest}$. (1+z)
Hubble's Law:	D $\simeq$ v / $H_o \simeq$ (c/H_o) . z = R_o . z
Item:	Numbers inside R_0=(c/H_0)$\simeq$13.7 Glyr:
Photons:	$N_{h\nu} \sim 10^{89}$
Baryons:	$N_b \sim 10^{80}$
η=Photons/Baryons	$\eta \sim 10^9$
Energy Density:	As fraction of critical closure density:
Baryons:	$\Omega_b = \rho_b/\rho_{crit} \simeq 0.042$
Dark Matter:	$\Omega_d = \rho_d/\rho_{crit} \simeq 0.23$
Dark Energy:	$\Omega_\Lambda = \rho_\Lambda/\rho_{crit} \simeq 0.73$
(Supermassive) black holes:	$\Omega_{smbh} = \rho_{smbh}/\rho_{crit} \simeq 0.0001$
Total	$\Omega_{Tot} = \rho_{Tot}/\rho_{crit} \simeq 1.00 \pm 0.02$
	($\rho_{crit} \simeq 10^{-29}$ gr/cm^3)

(0) Integrated EM Background: almost a power-law over $\lesssim$30 dex in λ!

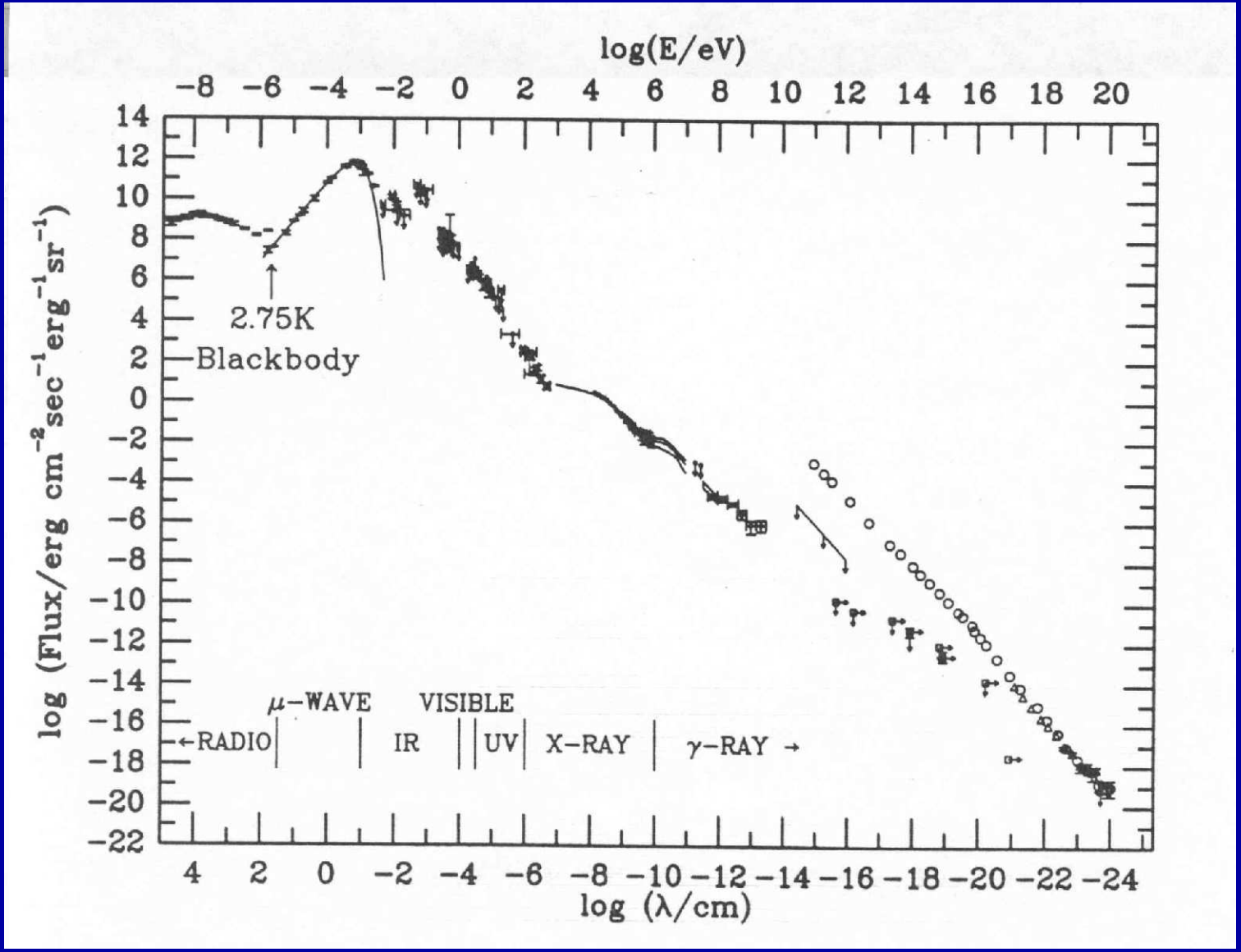

(Except for CMB), most photons in universe are produced by weak AGN and faint star-forming objects. Both have an N(z) that peaks at z$\simeq$1–2.

$\Rightarrow$ Most (radio) photons in Universe at z$\lesssim$6 generated by $<$1% of mass!

Distant Galaxies in the Hubble Ultra Deep Field
Hubble Space Telescope • Advanced Camera for Surveys

NASA, ESA, R. Windhorst (Arizona State University) and H. Yan (Spitzer Science Center, Caltech)

STScI-PRC04-28

Hubble UltraDeep Field: mapped Galaxy Assembly from $z \simeq 6$ to $z \simeq 0$.

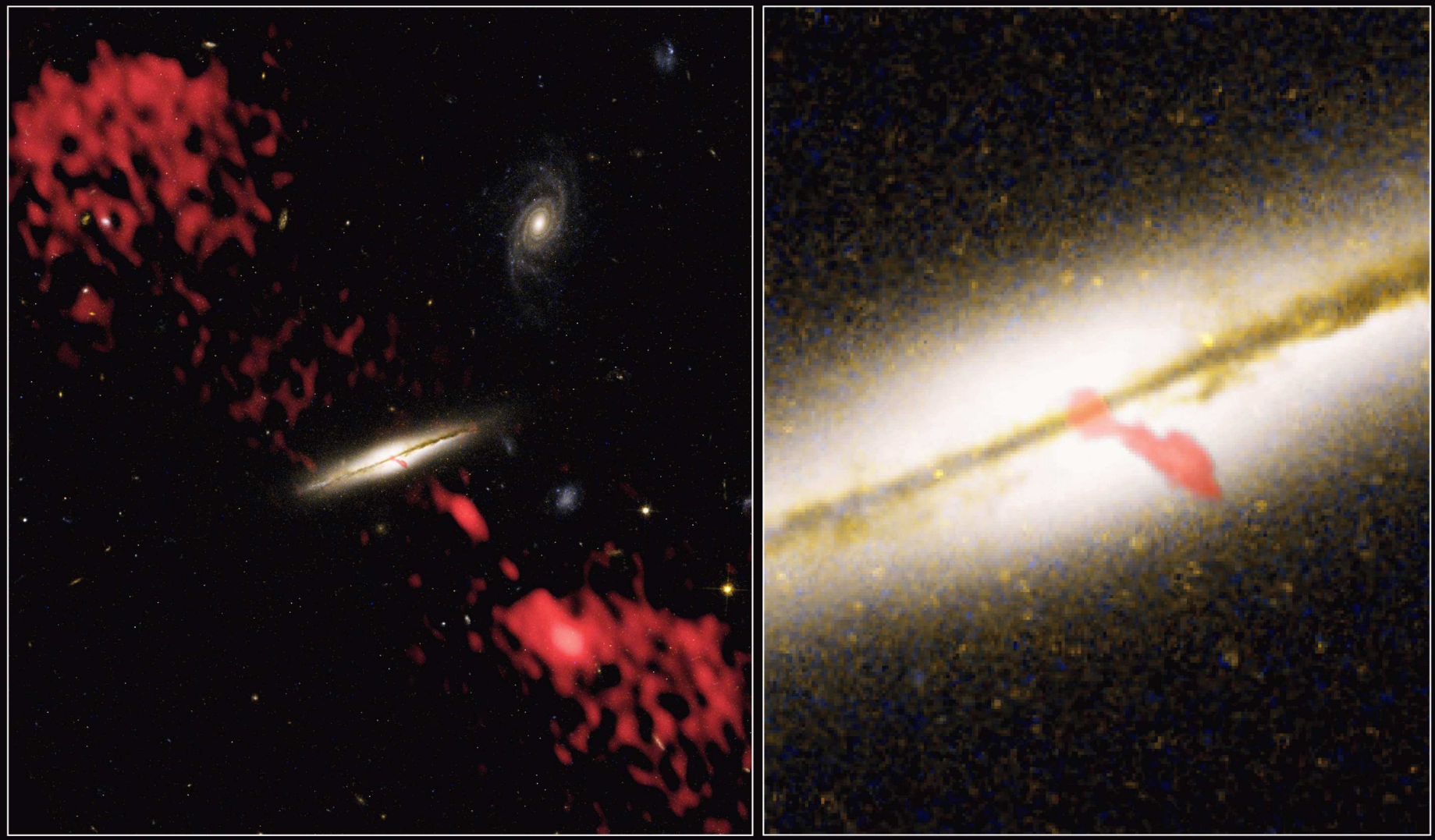

Radio Galaxy 0313-192

Hubble Space Telescope ACS WFC ▪ **Very Large Array**

NASA, NRAO/AUI/NSF and W. Keel (University of Alabama) ▪ STScI-PRC03-04

HST+VLA image of 0313-192: optical galaxy (color) and radio source (red).

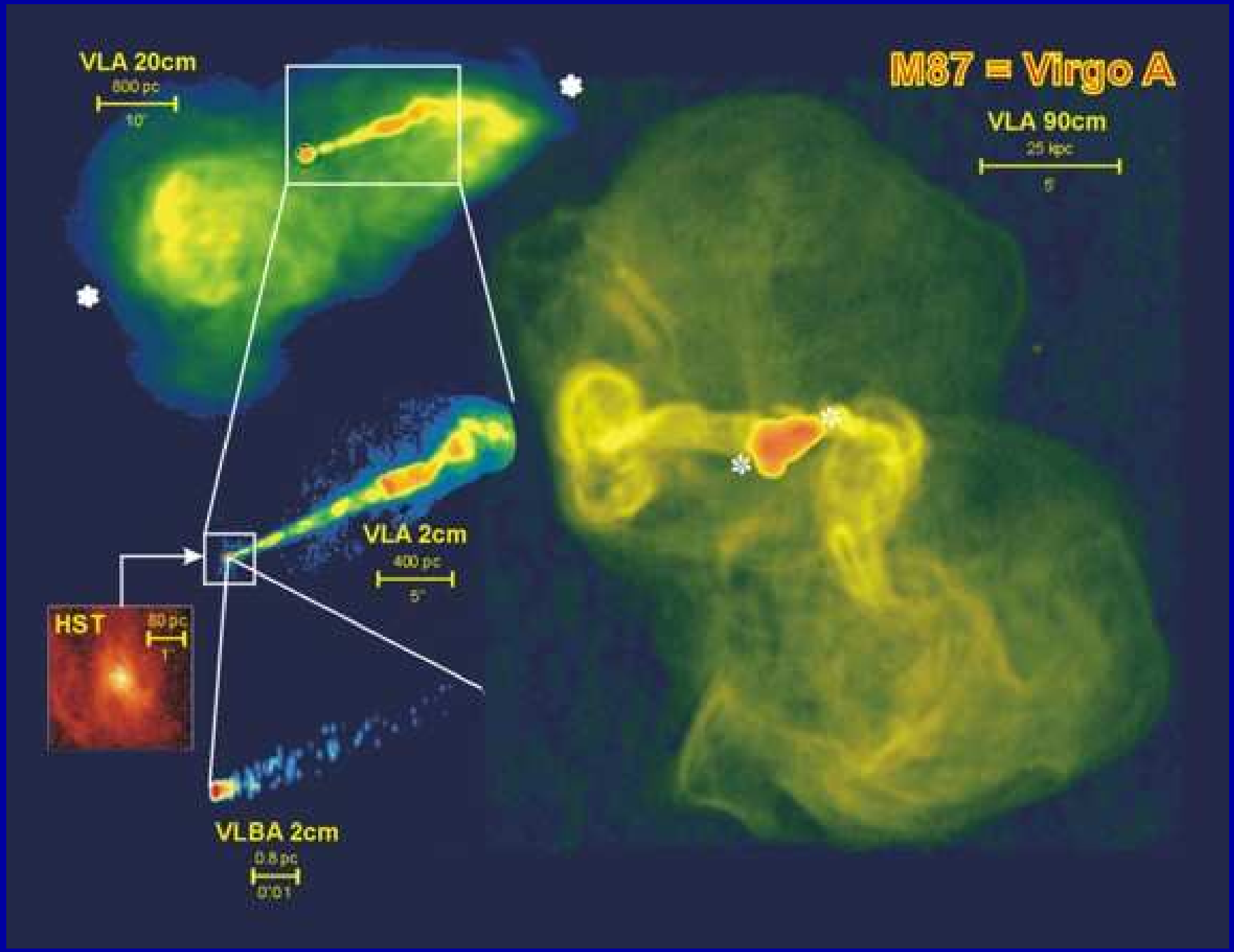

- VLA image of M87: Radio source stretches over a factor of 30,000 in size.
  - Supermassive black-hole powered sources are brightest in the universe.

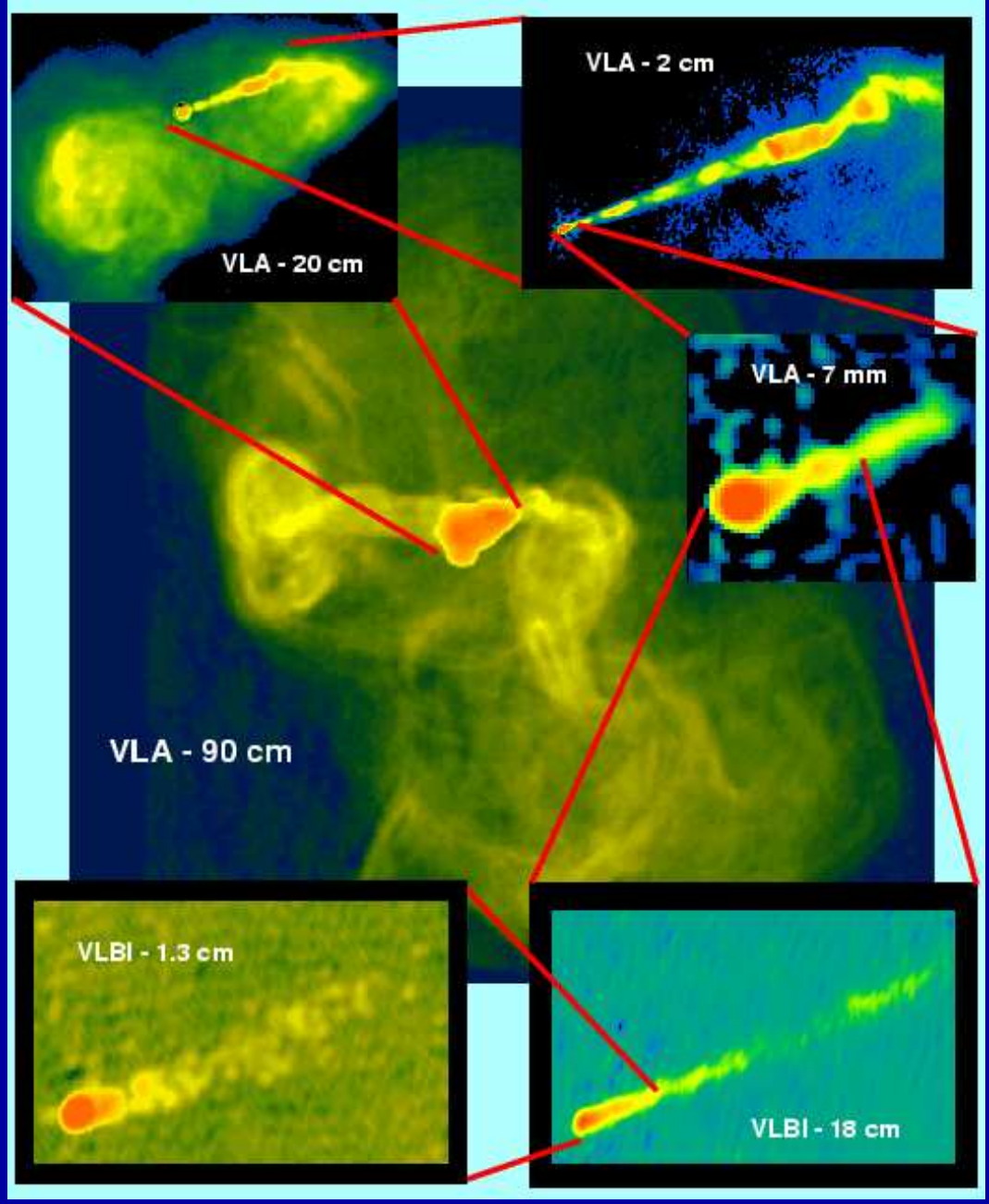

- VLA/VLBI image: M87 radio source stretches over factor 300,000 in size.
- Jets in AGN have a fantastic memory for direction: $\lesssim 0.3$—$\gtrsim 10^5$ years.

HST and NRAO papers by F. Machetto et al., J. Biretta et al., F. Owen et al.

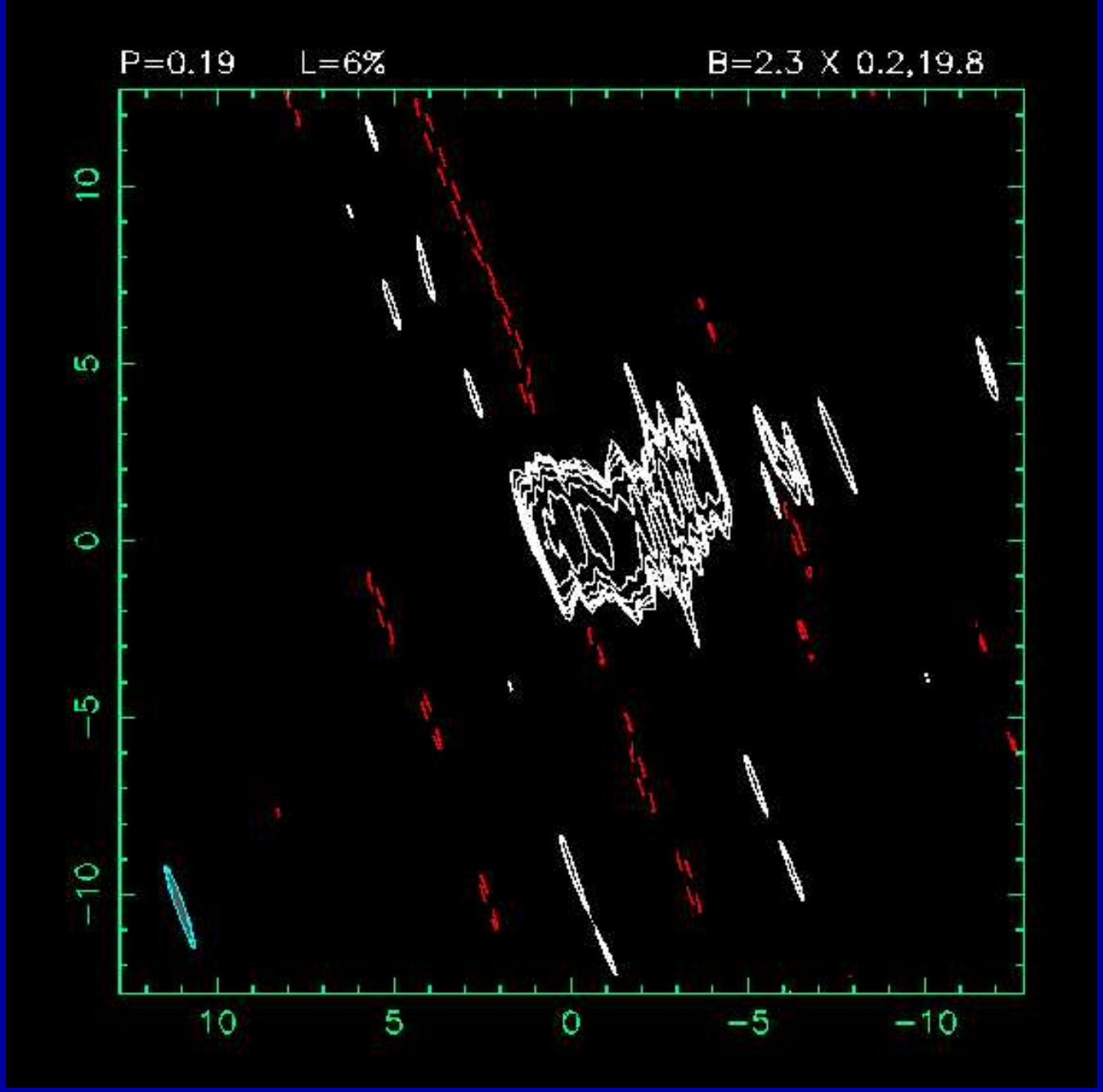

- (Orbiting) Very Long Baseline image of M87: radio jet covers 8 dex in size.
- Jets in AGN have a fantastic memory for direction: $\lesssim 10^{-3}$–$\gtrsim 10^{5}$ years.

Orbiting VLBI by Hirabayashi et al. 2000, Pub. Astr. Soc. Jap., 52, 997

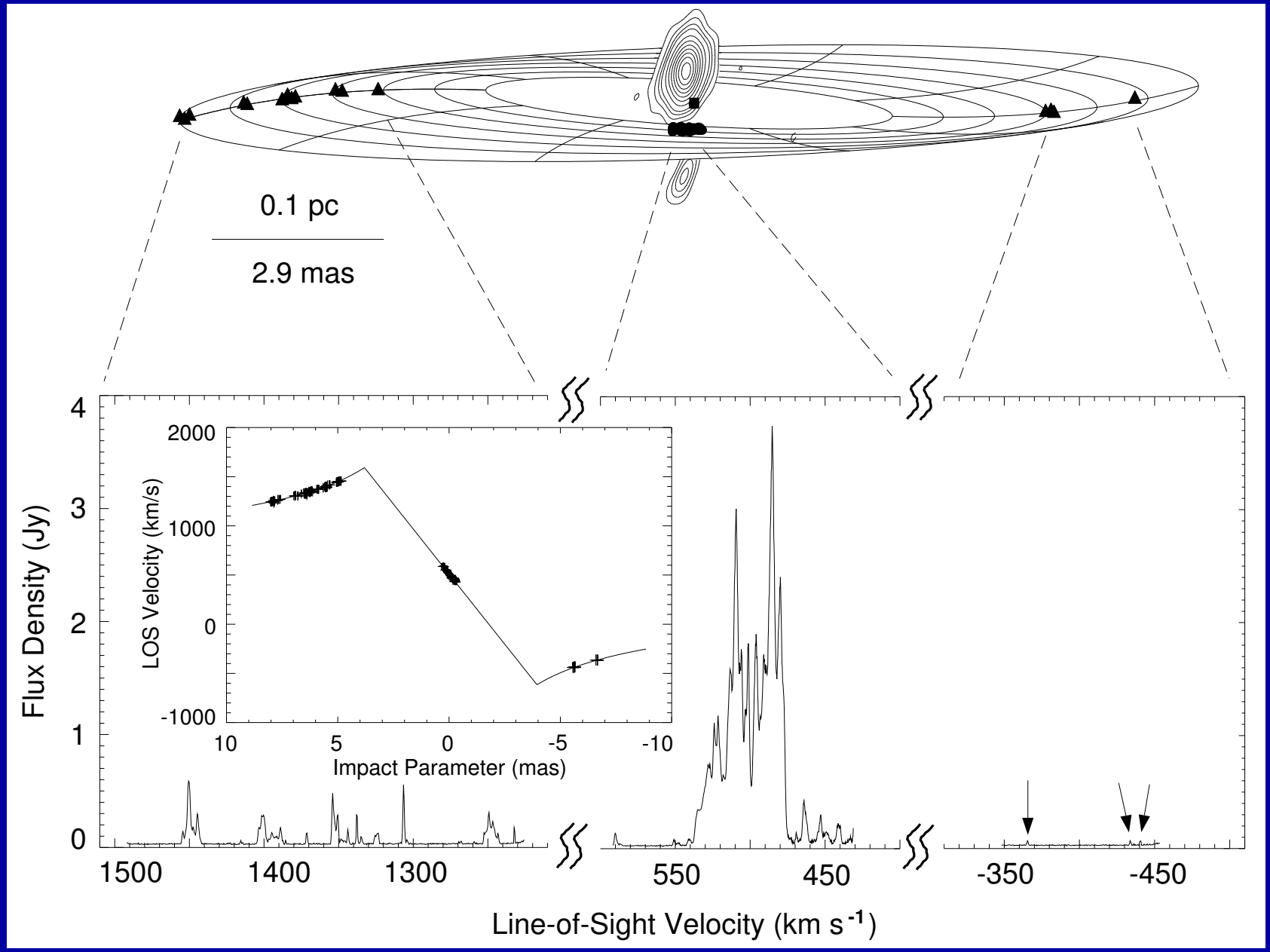

Geometric distance to NGC 4258 based on Kepler's 3rd law: 7.2±0.3 Mpc

$\Rightarrow$ Precise distance and mass: 23.5±1.0 Mly, $M_{smbh} \simeq 10^{7.59\pm0.04}\ M_\odot$

(J. R. Herrnstein et al. 1999, Nature, 400, 539)

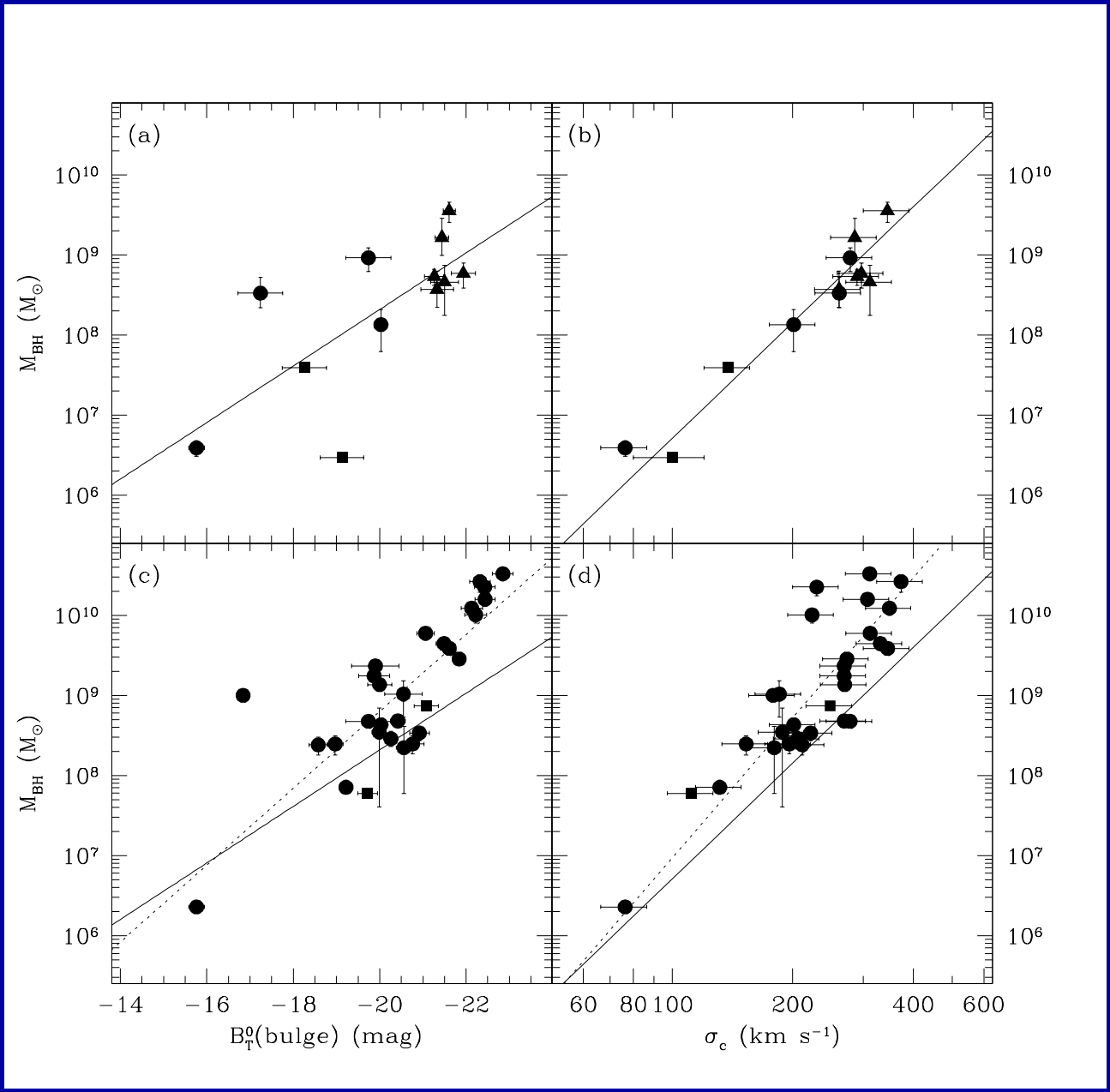

SMBH mass vs. bulge-mass relation, measured via velocity dispersion $\boldsymbol{\sigma}$.

On average: $M_{\boldsymbol{bulge}} \simeq 10^{11}\ \boldsymbol{M_\odot}$ produces $M_{\boldsymbol{smbh}} \simeq 10^{\boldsymbol{8.3}}\ \boldsymbol{M_\odot}$

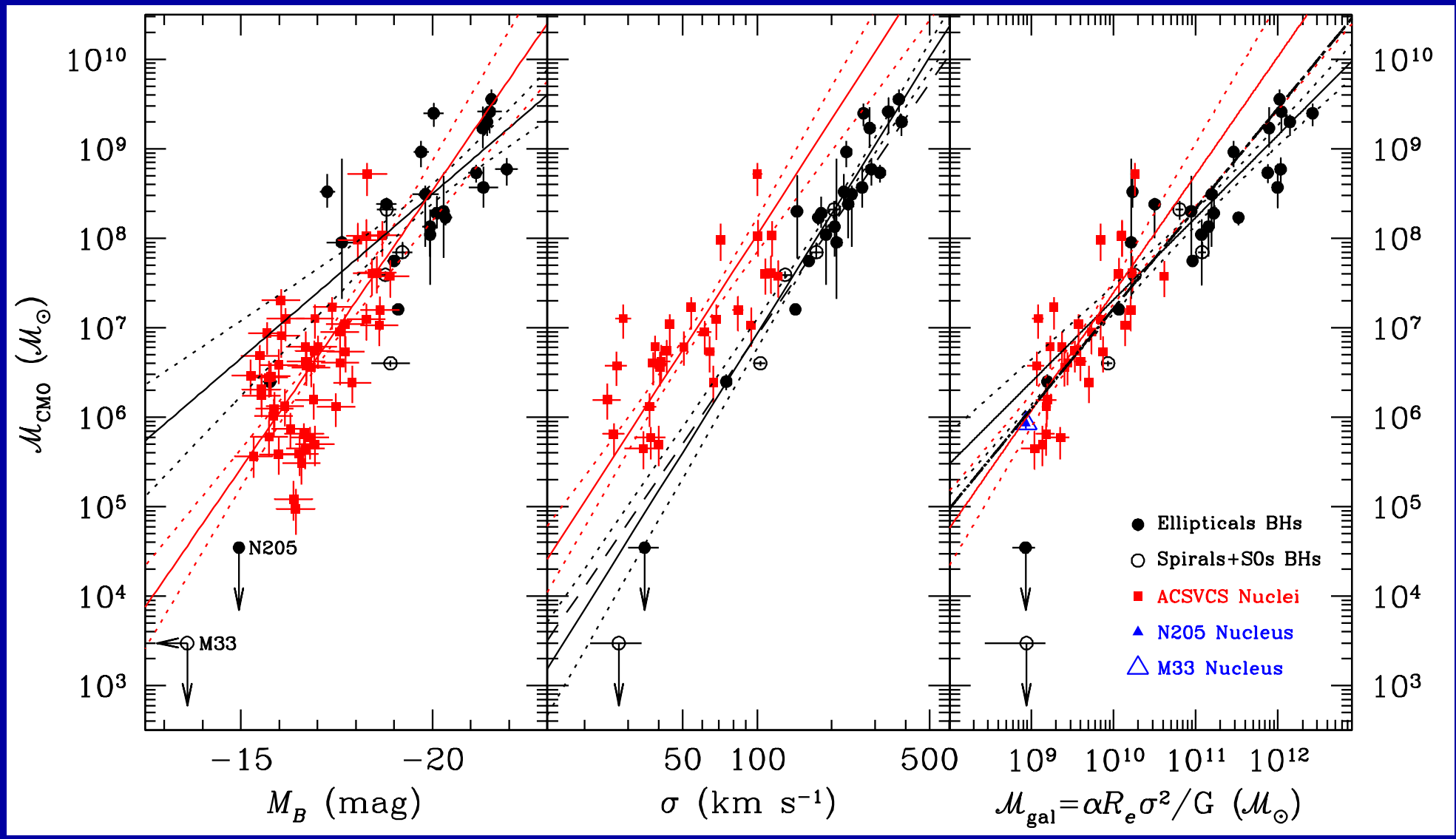

SMBH mass vs. bulge-mass relation, measured via corrected velocity dispersion σ

On average: $M_{bulge} \simeq 10^{11}\ M_\odot$ produces $M_{smbh} \simeq 10^{8.3}\ M_\odot$

$\Rightarrow$ On average, 0.2% of galaxy bulge mass ends up in central SMBH!

HST and Keck-AO near-IR images of luminous radio galaxy Cen-A (G. Canalizo et al., 2003, ApJ, 597, 823). Central AGN likely triggered by a minor merger seen in this image (secondary knot at 4 o'clock).

CARDINAL QUESTIONS: If all galaxies formed by hierarchical mergers, and SMBH's grew hierarchically as well:

- How exactly did go SMBH growth keep pace with galaxy assembly?
- And how do we observe this (since we don't live long enough)?

Note: Growing a $\sim$100 $M_\odot$ Pop III star BH at z$\sim$15 into a 10^9 $M_\odot$ SMBH at z=0 takes 23 equal-mass mergers, or one every 0.58 Gyr.

Active Galactic Nuclei: powered by supermassive black-holes (10^6–10^{10} $M_\odot$)

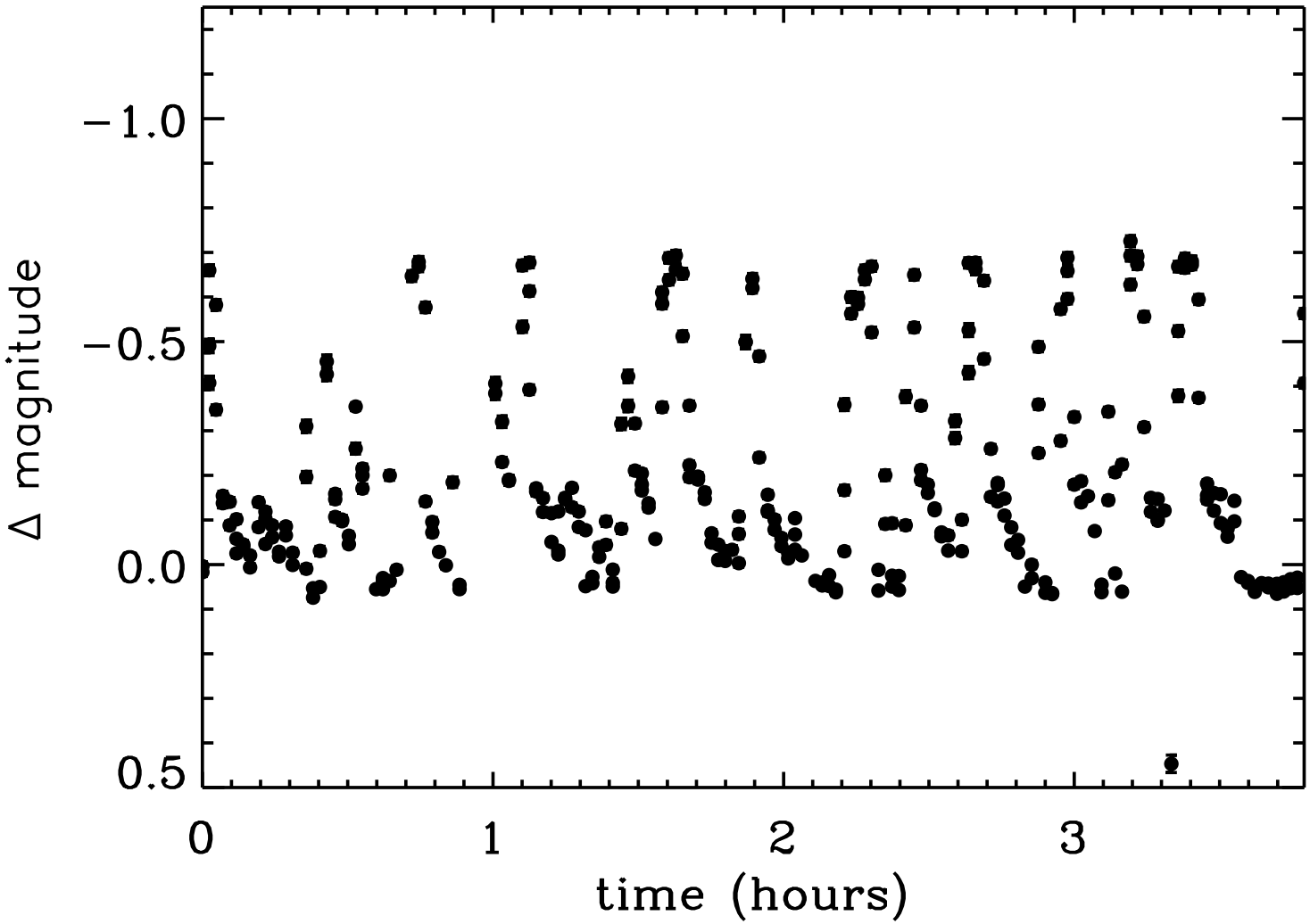

Light curve of the AGN Mrk421 with a super-massive black hole in its center.

(Quasi-periodic) variability on time-scales of 0.3 hr: $M_{smbh} \lesssim 6 \times 10^7 M_{sun}$.

Active Galactic Nuclei: powered by supermassive black-holes (10^6–10^{10} $M_\odot$)

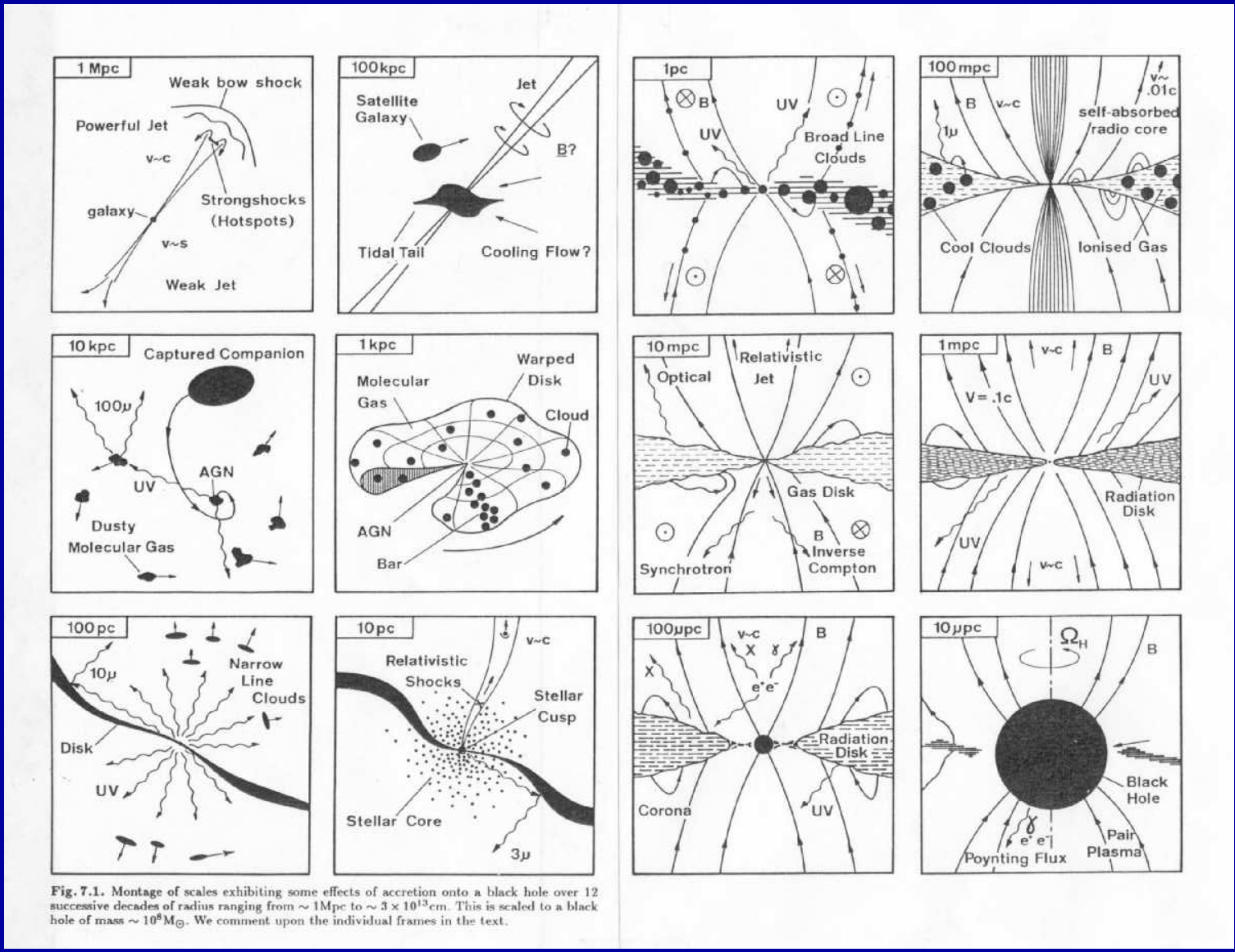

Fig. 7.1. Montage of scales exhibiting some effects of accretion onto a black hole over 12 successive decades of radius ranging from ~ 1Mpc to ~ 3×10^{13}cm. This is scaled to a black hole of mass ~ $10^8 M_\odot$. We comment upon the individual frames in the text.

Affect surroundings over 12 dex in size: from AU to Mpc scales (300 Mlyr),

or from General Relativistic Singularity (AU) to Relativistic Jets (Mpc).

If jet shines in your face $\Rightarrow$ Quasar: $10^{15} L_\odot$ coming from several AU!

(1) Scientific Background and Goals

• The HST Ultra Deep Field (HUDF) is the deepest field ever taken. It covers 400 orbits, approximately over 4 epochs each about 1 month apart.

• The combined HUDF detection limit is AB=29.1 mag (= 10 nJy = 10^{-34} W/m^2/Hz; 10-σ). For each of these 4 epochs it is AB$\gtrsim$28.0 mag.

GOAL 1: Unique opportunity for faint variability study on months timescales.

• The HUDF shows a plethora of faint galaxy morphologies/structure also seen in the Deep Fields, but at much higher S/N. A large number of "tadpole" galaxies is seen: highly elongated AND asymmetric galaxies.

• Cowie et al. (1995, 1996)'s first noted chain galaxies. They may be early stage mergers, like Luminous Diffuse Objects (Conselice 2004) or "clump-clusters" (Elmegreen et al. 2004). They have no nearby counterparts.

GOAL 2: Study tadpole galaxies in HUDF and find clues to their nature, redshift distribution, and epoch dependent merger rate.

TADPOLE GALAXIES IN THE *HUBBLE ULTRA DEEP FIELD*

Amber N. Straughn, Seth H. Cohen, Russell Ryan, Nimish P. Hathi, Rogier A. Windhorst

Department of Physics and Astronomy, Arizona State University, Tempe, AZ 85281; amber.straughn@asu.edu

Bahram Mobasher and other GRAPES co-authors (TBD)

Space Telescope Science Institute, 3700 San Martin Drive, Baltimore, MD 21210

and Anna Pasquali, ETH, Zurich, Switzerland

Space Telescope Science Institute, 3700 San Martin Drive, Baltimore, MD 21210

ABSTRACT

The Hubble Ultra Deep Field ("UDF") presents a wealth of galaxies, some very oddly shaped. In particular, many galaxies that appear to have a bright knot at one end with an extended tail at the other. These objects are presumably in a dynamically unrelaxed state. In this paper, we systematically select these "tadpole galaxies" from the UDF and study them as a function of their photometric redshifts. We find that in general the redshift distribution of these tadpole galaxies follows the distribution of all galaxies in the UDF field. The ratio of tadpole galaxies to field galaxies is found to peak at a redshift of z$\sim$1.8, and the percentage of tadpole galaxies at this redshift is $\sim$2.7%. This is $\sim$3$\times$larger than the percentage of variable galaxies found in the Hubble Deep Field in a similar redshift region. Further study should be performed on these tadpole galaxies to determine if they are in fact variable and contain (hidden) AGN.

Subject headings: galaxy mergers: general — Hubble UltraDeep Field — cosmology

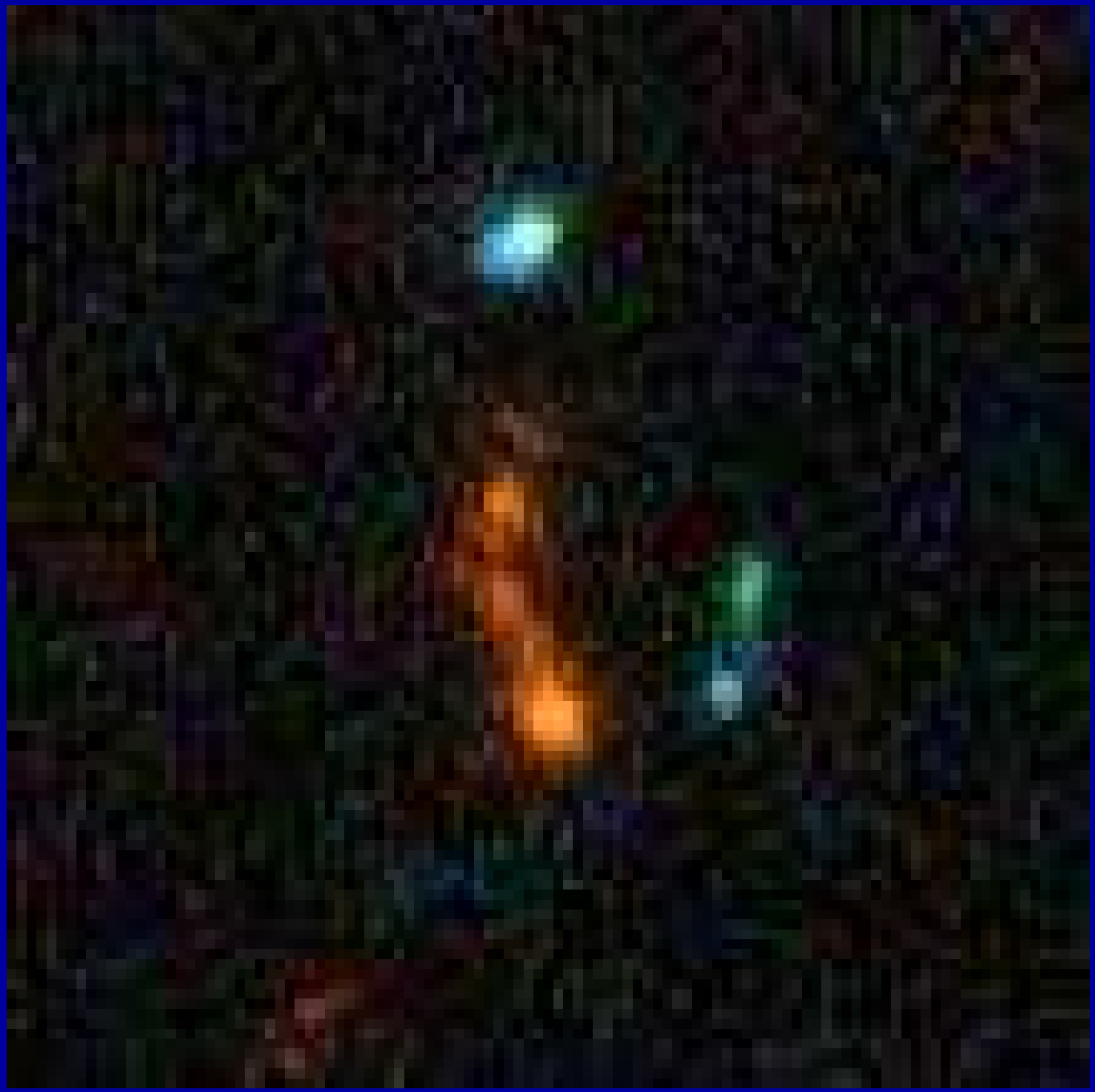

Rhoads et al. 2005, ApJL, 621, 582 (astro-ph/0408031): Tadpole at z=5.49.

(2) A study of Tadpole Galaxies in the HUDF

- Many of these tadpole galaxies have a bright knot at one end with an extended tail at the other, and often two un-centered knots.

- They are presumably dynamically unrelaxed, early-stage mergers.

We select them as following:

(A) Make a lowly de-blended object catalog and find all highly inclined systems $\Rightarrow$ first pass of tadpole candidates or "tails".

(B) Make a highly de-blended object catalog and find all clumps rounder than a certain limit located inside sample (A) that are:

(1) Dislocated from the tail's geometric center by a certain amount, AND

(2) Not displaced in position angle from the tail's major axis by more than a certain amount.

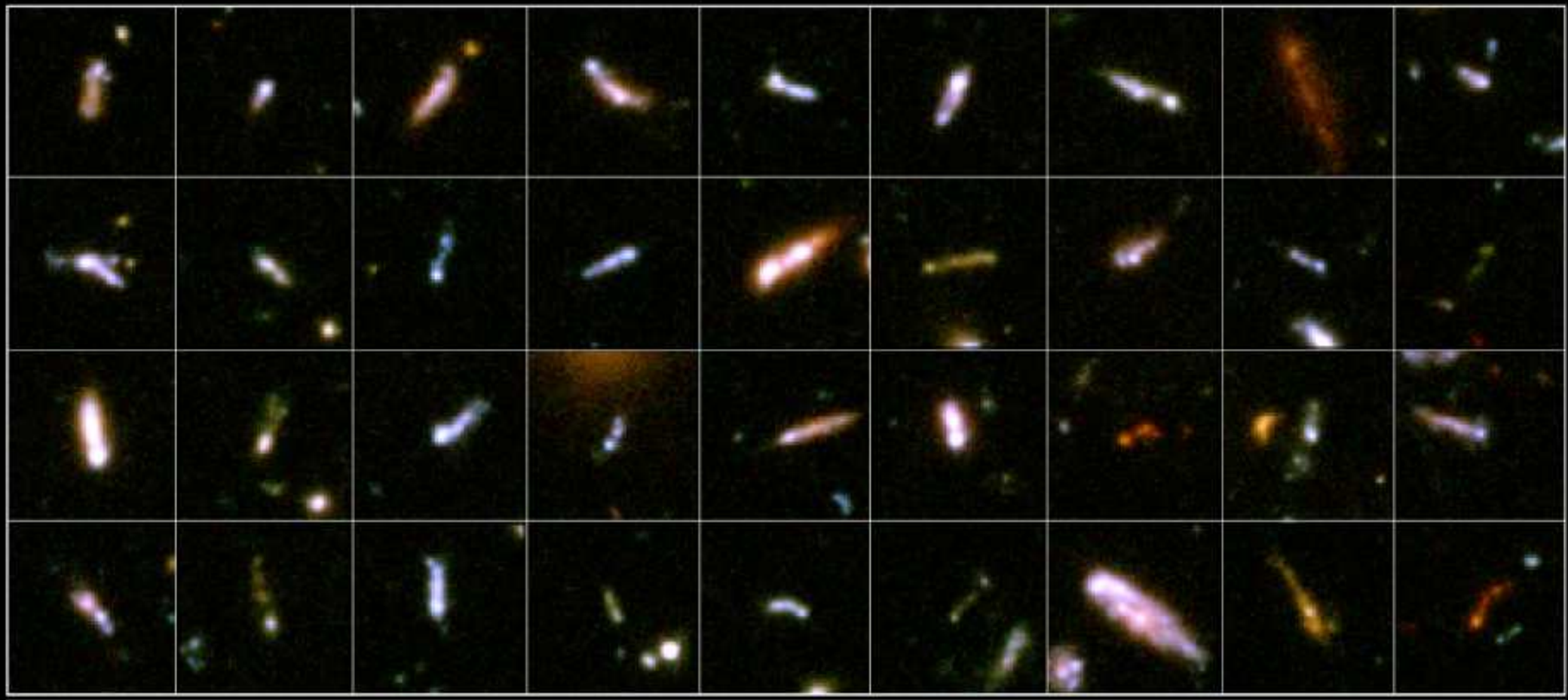

"Tadpole" Galaxies in the Hubble Ultra Deep Field
Hubble Space Telescope ▪ ACS/WFC

NASA, ESA, A. Straughn, S. Cohen and R. Windhorst (Arizona State University), and the HUDF team (STScI) STScI-PRC06-04

Tadpole galaxies in press release: hubblesite.org/newscenter/archive/2006/04/

Straughn, A. N., et al. 2006, ApJ, 639, 724 (astro-ph/0511423)

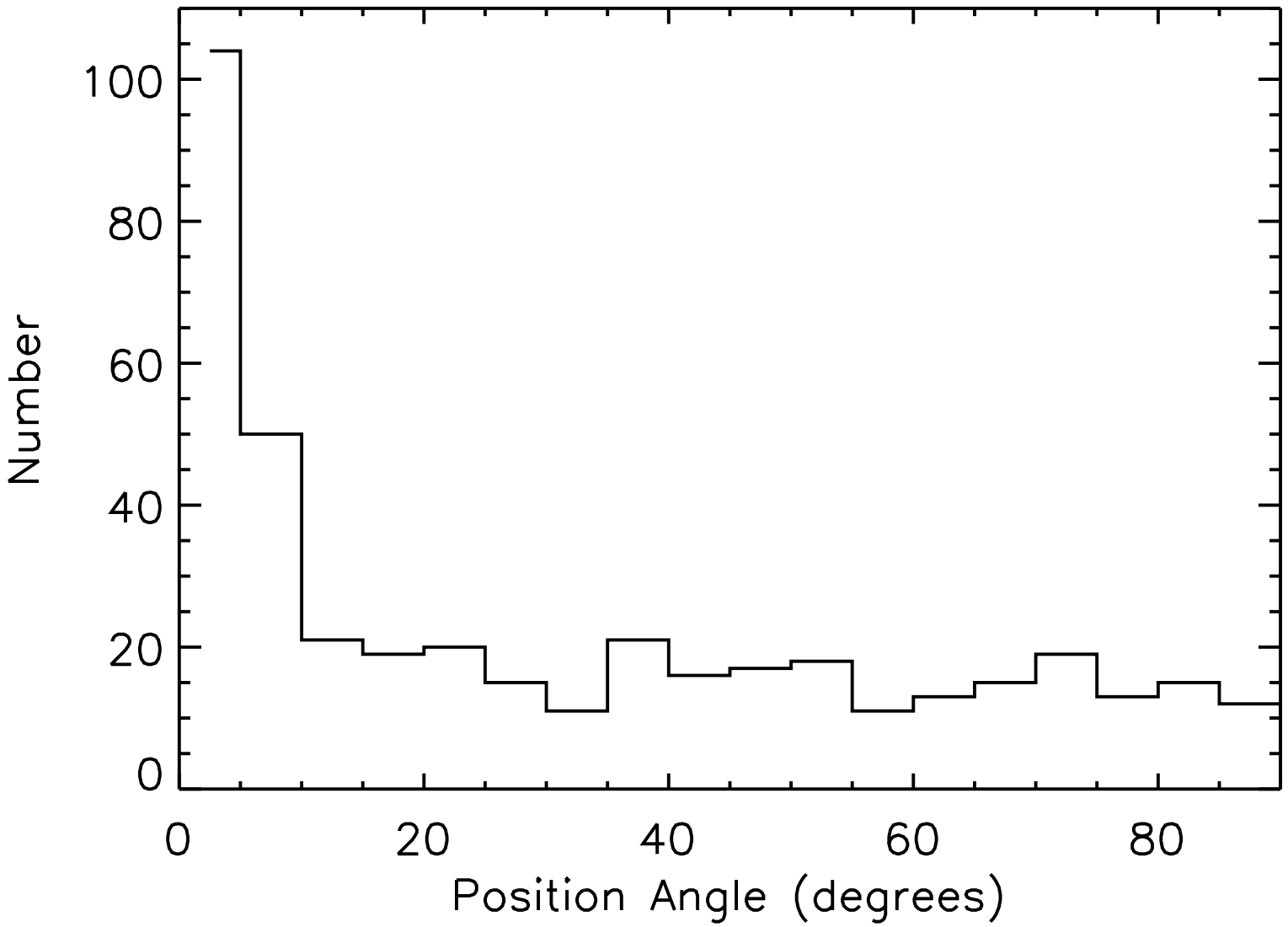

ΔPA(off-axis knot—tail) distribution of tadpole galaxies in the HUDF:

- Clear excess of knots at $|\Delta\mathrm{PA}| \lesssim 10$ deg.

$\Rightarrow$ Most tadpoles are likely real, rather than chance superpositions.

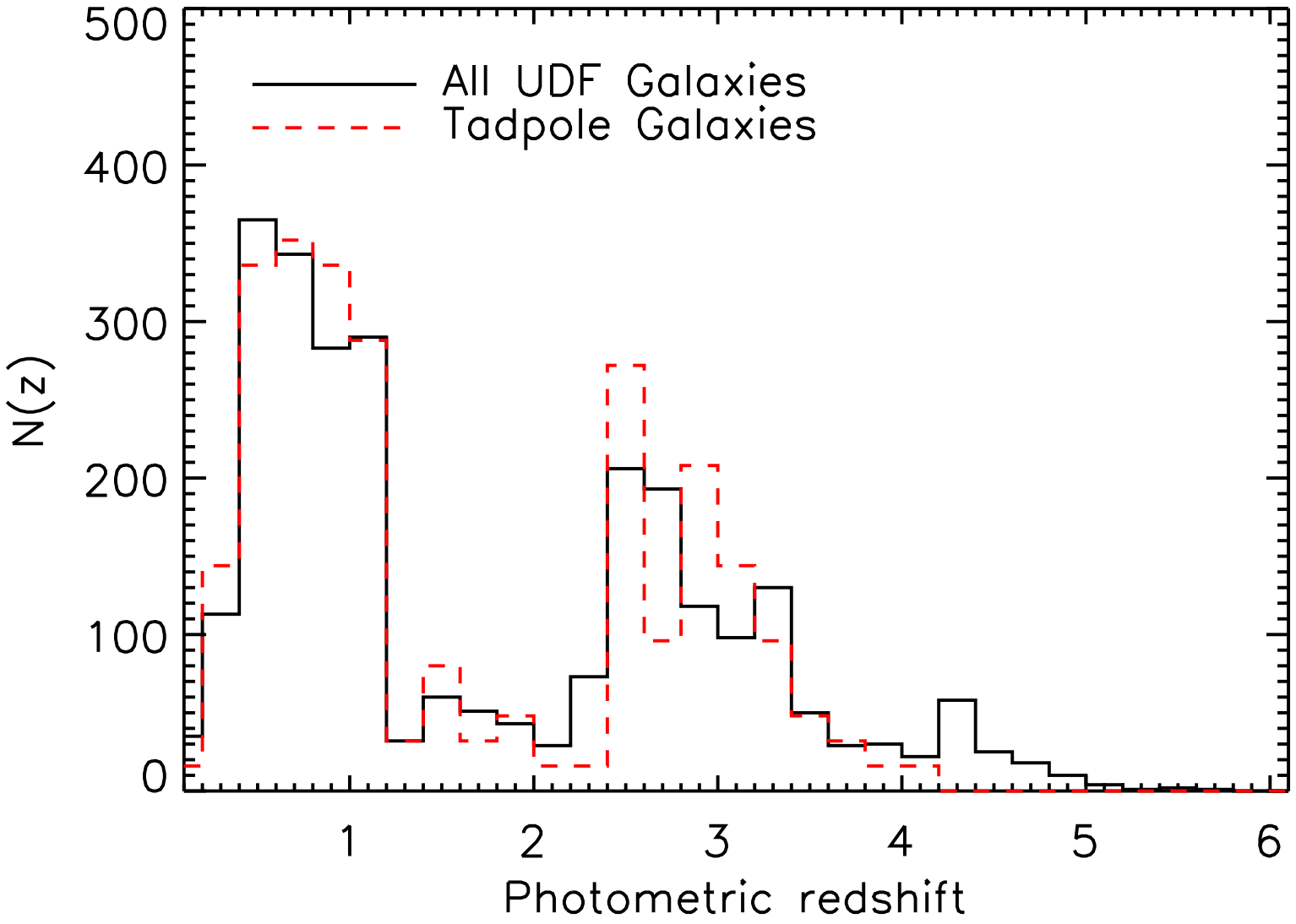

BViz(JH) photo-z distribution of galaxies in the HUDF:

Full drawn: all HUDF field galaxies.

Dashed: HUDF tadpole galaxies ($\times 16$ for comparison with field galaxies).

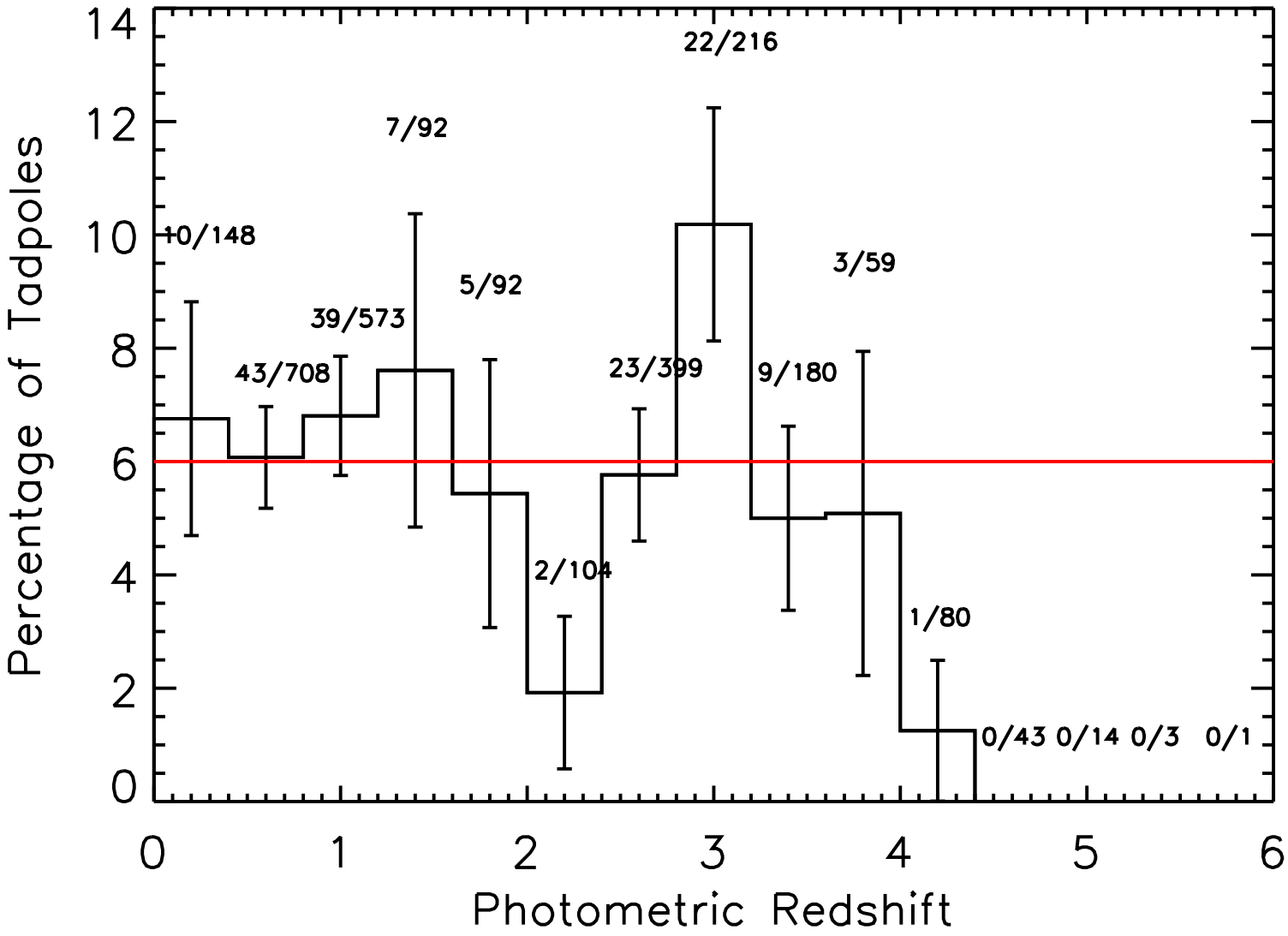

Fractional redshift distribution of tadpoles compared to all HUDF galaxies.

- To first order, shape of tadpole galaxy redshift distribution is the same as that of field galaxies: average $N(z)_{tadpoles} \simeq 6\% \; . \; N(z)_{field}$.

(2) Summary of Tadpole Galaxies in the HUDF

The tadpole photo-z distribution follows the N(z) of all HUDF galaxies, which peaks at z$\sim$1–2. Tadpole fraction is $\sim$6% of all HUDF galaxies.

Each tadpole is $\sim$1"$\simeq$8 kpc across. At the median z$\sim$1.5, these objects are $\sim$3.6 Gyr old if born at z$\sim$7. If each clump in a tadpole has M$\sim 10^8$–$10^9\ M_\odot$ then τ(merging) is $\lesssim 10^8$ years ($\lesssim$few% of the galaxy lifetime).

$\Rightarrow$ If each galaxy underwent a few $\sim$equal mass (major) mergers during its lifetime, $\sim$6% of HUDF all galaxies could be seen as tadpoles.

- Majority of tadpoles likely not edge-on disk galaxies, but rather linear structures of "sub-galactic clumps" on moving past/through each other.
- Did the merger rate peak at z$\sim$1–2, before effects from Λ kicked in?
- Was Λ itself responsible for dramatically winding down the epoch dependent merger rate at z$\lesssim$0.5–1?

Clues to Galaxy Formation from Variable Objects In The Hubble Ultra-Deep Field

Seth H. Cohen, Russell E. Ryan Jr., Nimish P. Hathi, Rogier A. Windhorst

Department of Physics and Astronomy, Arizona State University, Tempe, AZ 85287-1504

seth.cohen@asu.edu

A. Koekemoer, C. Xu, N Pirzkal, S. Malhotra, L. Strolger, other Grapes co-I's

Space Telescope Science Institute, Baltimore, MD 21218

and

Other People

Other Institute, Elsewhere, MD 21218

ABSTRACT

We present a photometric study of galaxies in the Hubble Ultra Deep Field by splitting the data into four sub-stacks of approximately equal exposure times. Variable objects are selected by studying the error distribution between different epochs and selecting $3 - -3.5\sigma$ outliers. The analysis is performed in both the i' and z' bands separately and together. We find 337 objects in the i'-band, 222 in z'-band and 66 in the combined sample.

Subject headings: galaxies, variable objects

.

(3) A Study of Variable Objects in the HUDF

• Split the HUDF into 4 sub-stacks of ∼equal exposure times each ∼1 month apart. Treat both i' and z' bands separately as well as together.
The i'-band is so much deeper than z' that i'-band is the primary filter.

• Define significantly de-blended object apertures in total HUDF image. Use "dual input mode" to get **equal-aperture** fluxes in all epochs, using HUDF weight-maps for errors. Use also sliding box method.

• Use the error distribution between epochs to select $\gtrsim 3.0\sigma$ outliers.

• Among HUDF objects studied to i_{AB} =28.0 mag ($\gtrsim 10\sigma$), expect $\lesssim$13 bogus detections if the noise were purely Gaussian.
The noise is not entirely Gaussian, although the HUDF is as close to Gaussian as it gets in any astronomical CCD applications.

• ∼45 contain believable variable point sources at $\gtrsim 3.0\sigma$, most of which seen at $\gtrsim$2 epochs. Another 57 possibly variable candidates.

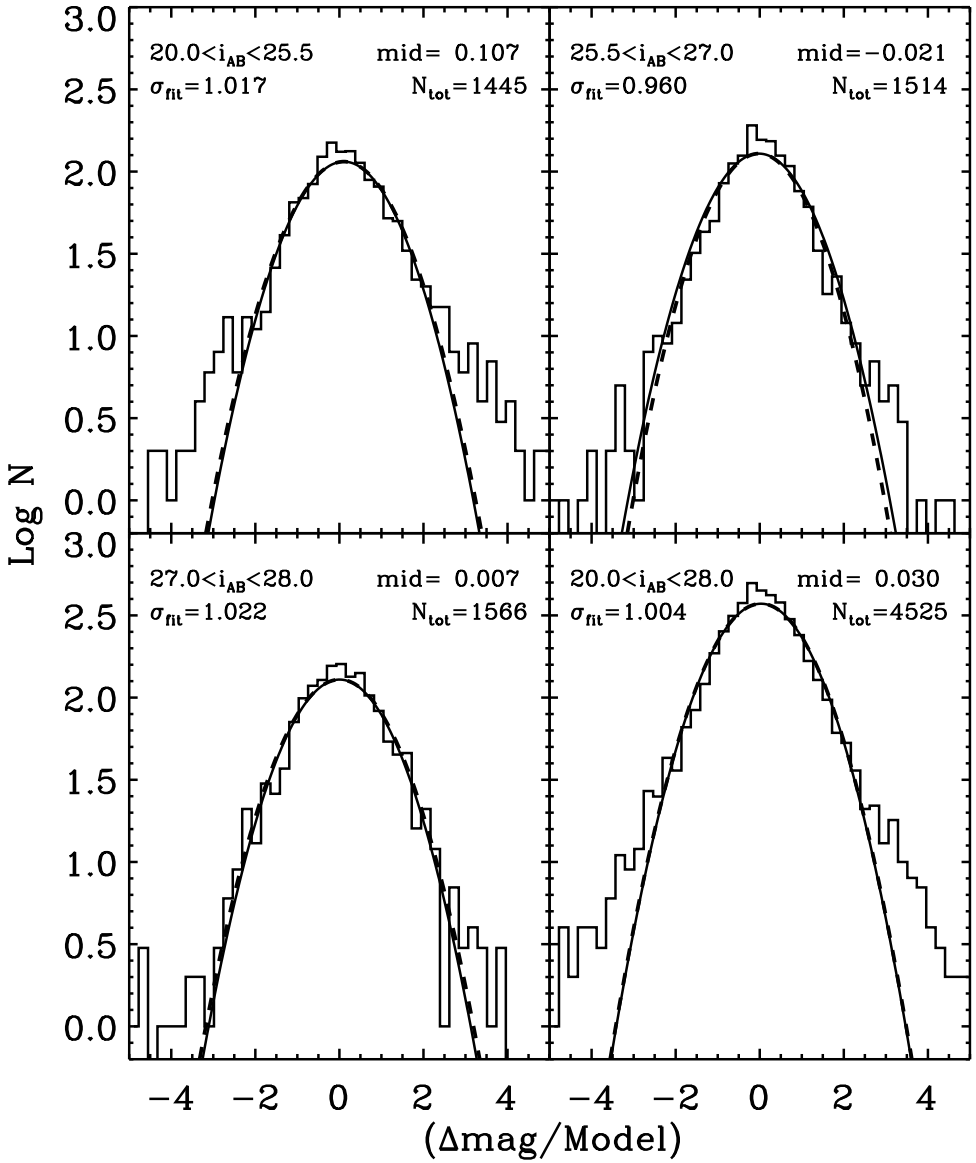

Is the HUDF noise really as Gaussian as it gets?

$\exists$ non-Gaussian noise at $\Delta\text{mag} \simeq 0 \Leftrightarrow$ CCD A/D-converter issue?

$\exists$ non-Gaussian noise at $|\Delta\text{mag}| \gtrsim 2\sigma \Leftrightarrow$ real variables and splitting issues

(3) Variable Objects in the HUDF:

Faint variable objects in HUDF could in principle be:

(1) Weak AGN.

(2) SNe in distant galaxies (see Strolger and Riess 2004).

(3) Perhaps Novae or other Long Period Variables in very nearby galaxies (only visible if $z \lesssim 0.03$)

(4) Faint high proper motion objects (KBO's, etc) [None found thus far].

$\Rightarrow$ Only (1) AGN and none of (2), (3), (4) were seen as variable objects in the HUDF thus far.

Cohen, S. H., et al. 2006, ApJ, 639, 731 (astro-ph/0511414)

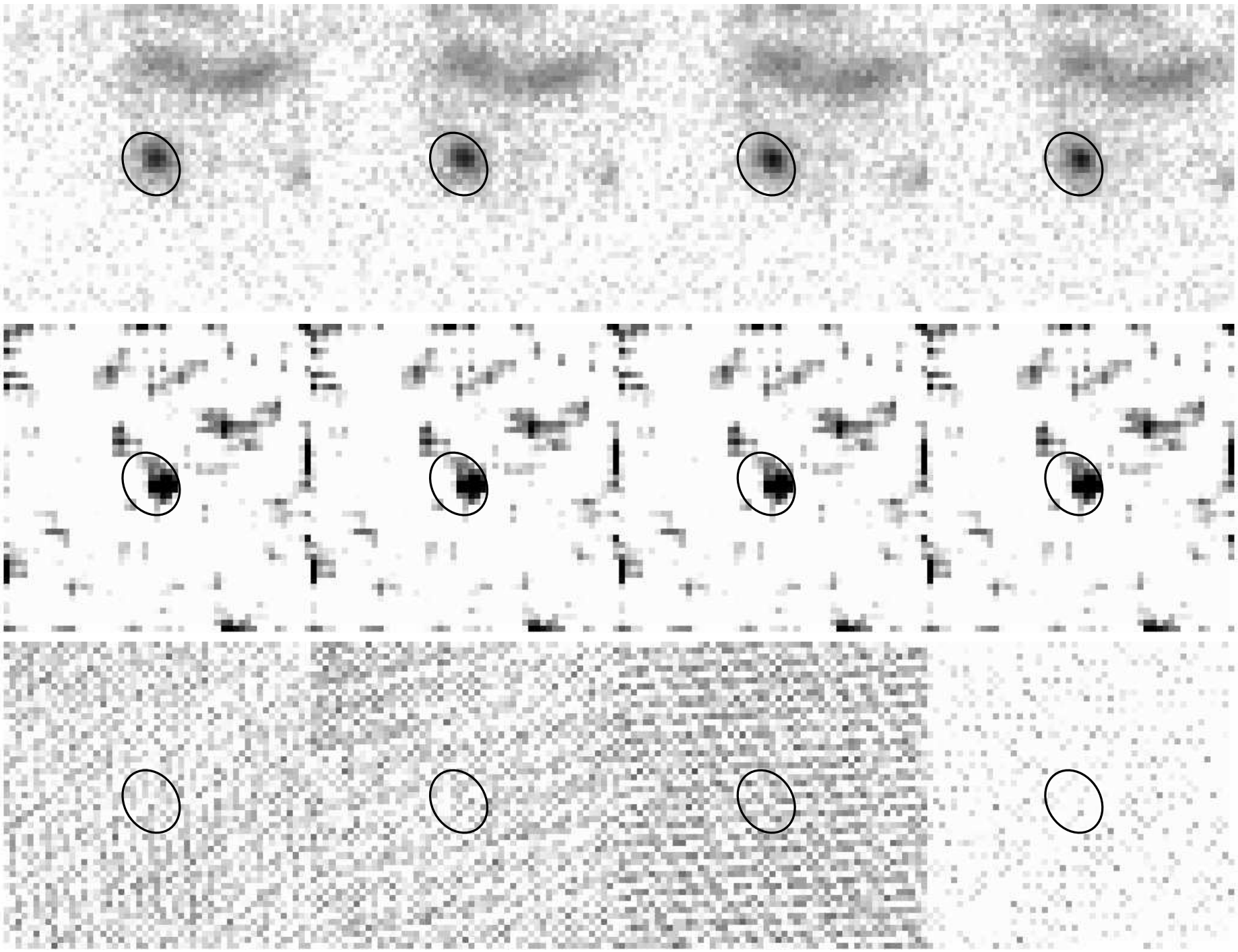

Top: 4 HUDF Epochs; Middle: 1 Variance map; Bottom: 4 Weight-maps.

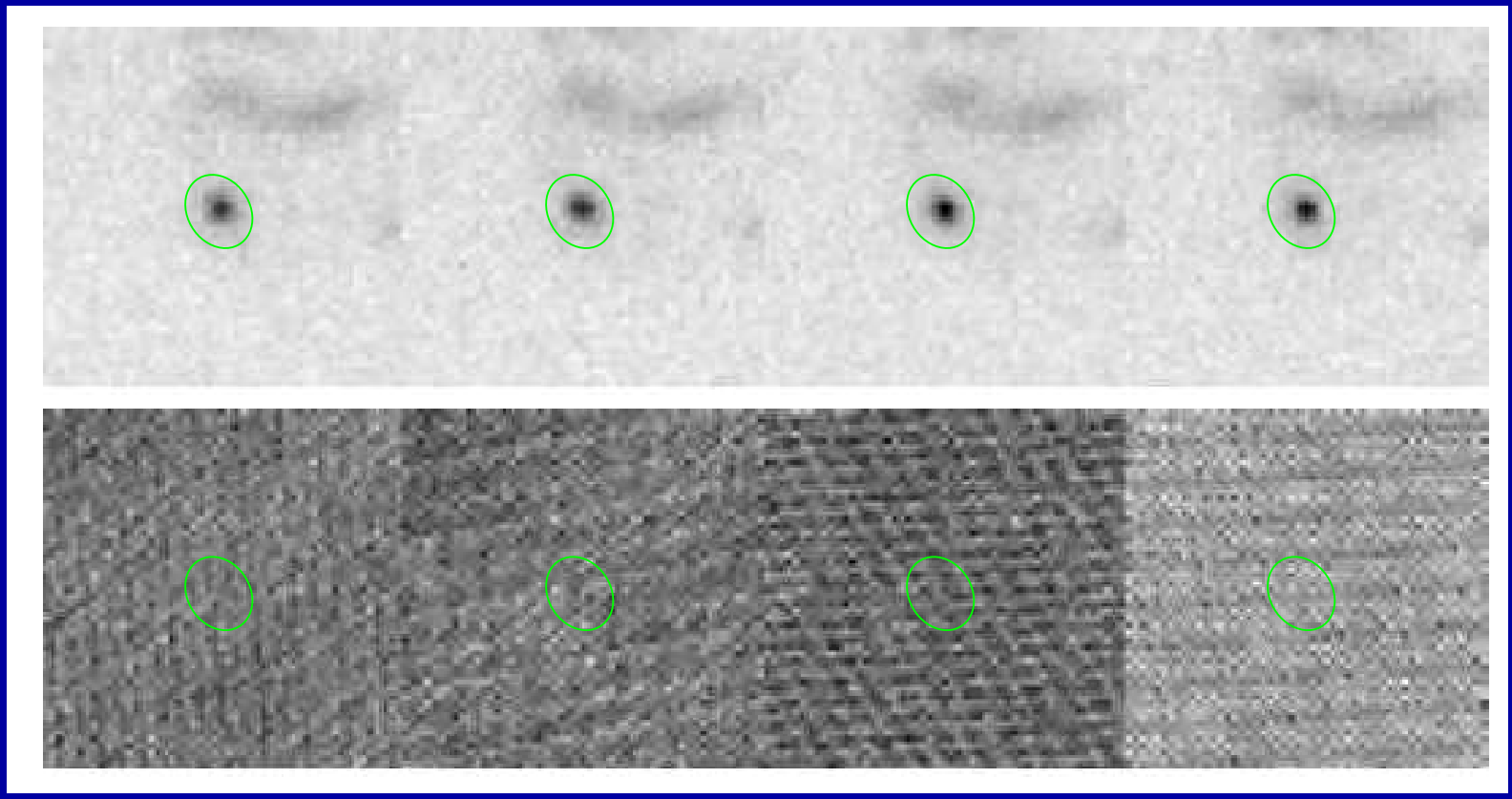

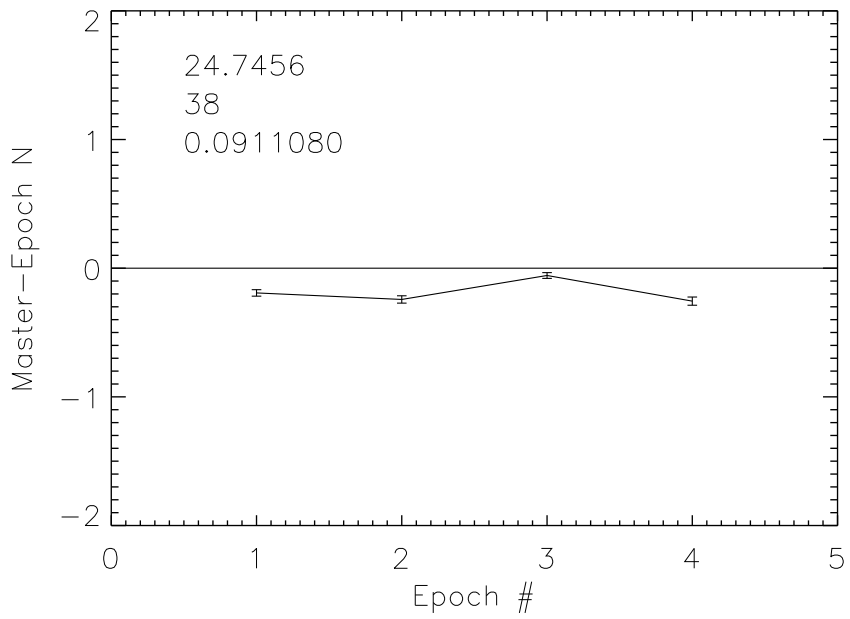

i'-Var Cand # 38 (z=1.122):

9% variability, AGN

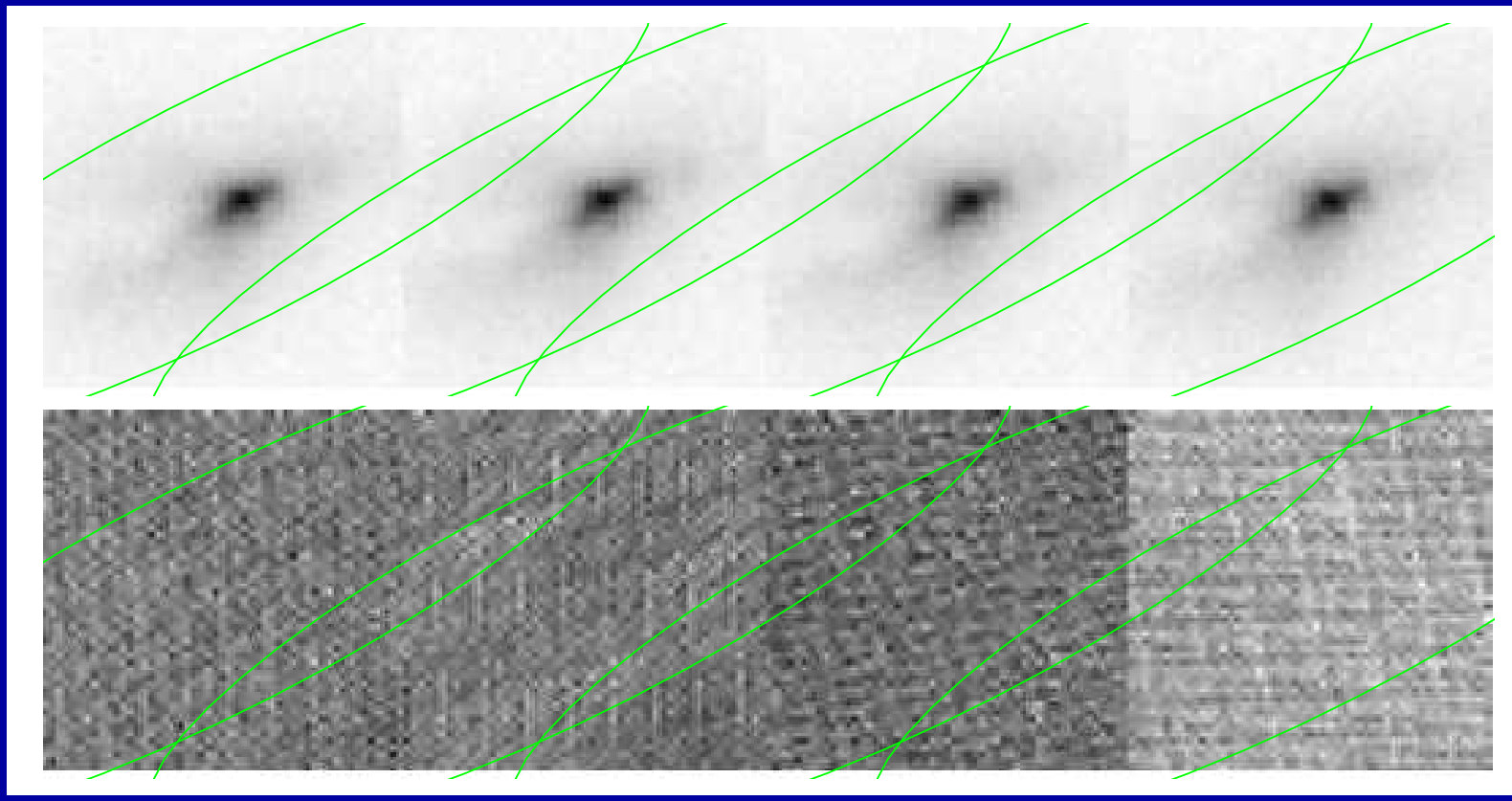

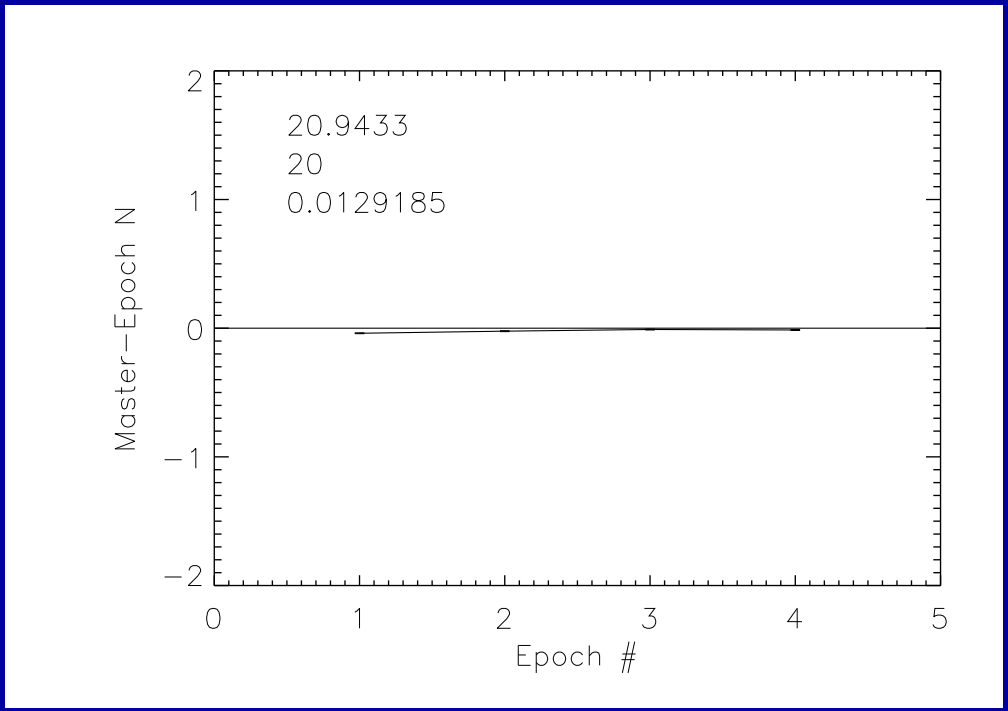

i'-Var Cand # 20 (z=0.906):

1% var (3-σ!), weak AGN

Faint Chandra X-ray source!
(Koekemoer et al. 2004)

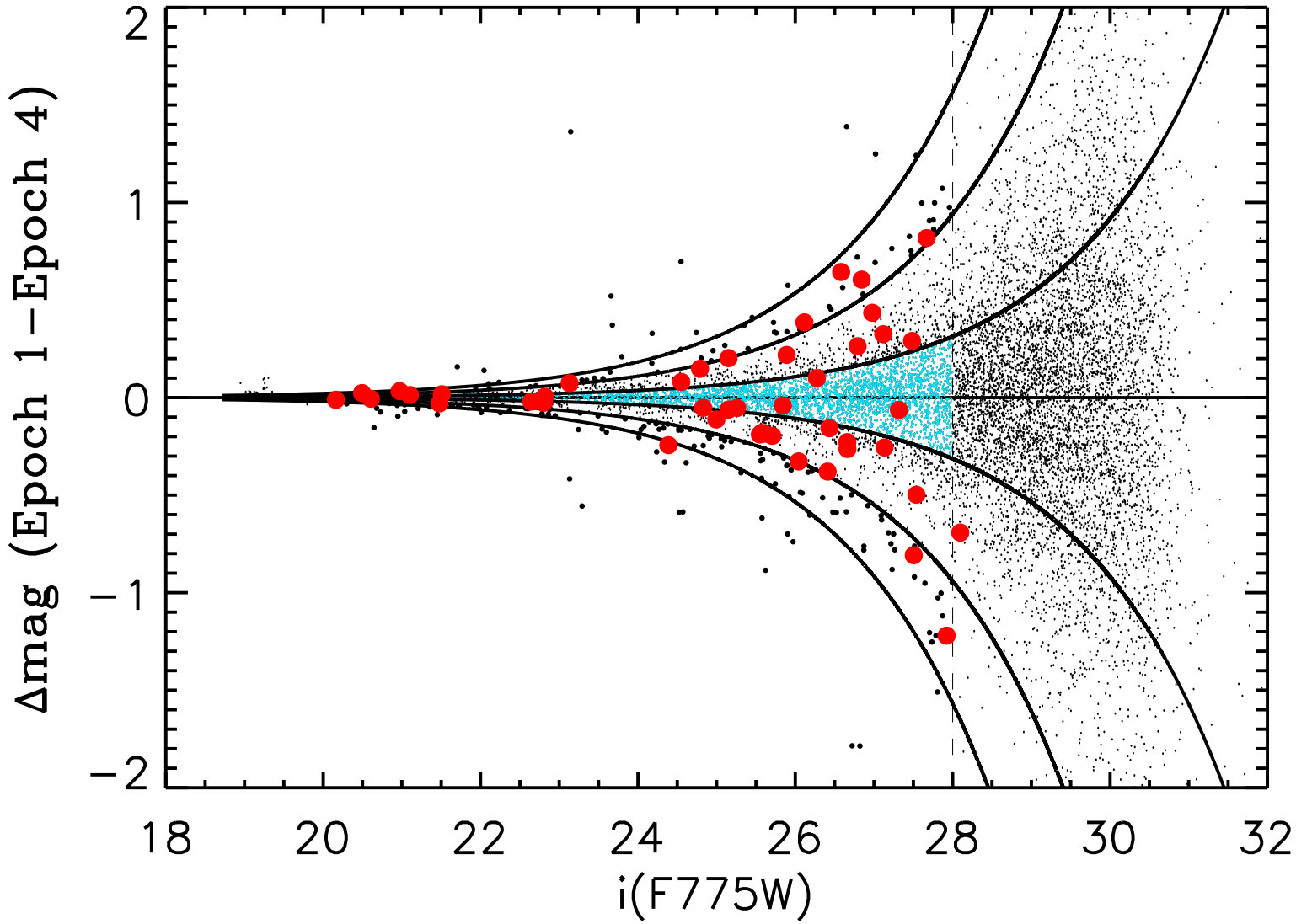

Flux ratio of all objects between two HUDF epochs plotted vs. total i-band flux. Lines are at $\pm 1.0\sigma$ (blue), $\pm 3.0\sigma$, $\pm 5.0\sigma$.

- All objects with |Delta mag| $\geq 3.0\sigma$ were inspected for plausible variability. This will yield $\lesssim 13$ bogus detections if the noise were purely Gaussian.

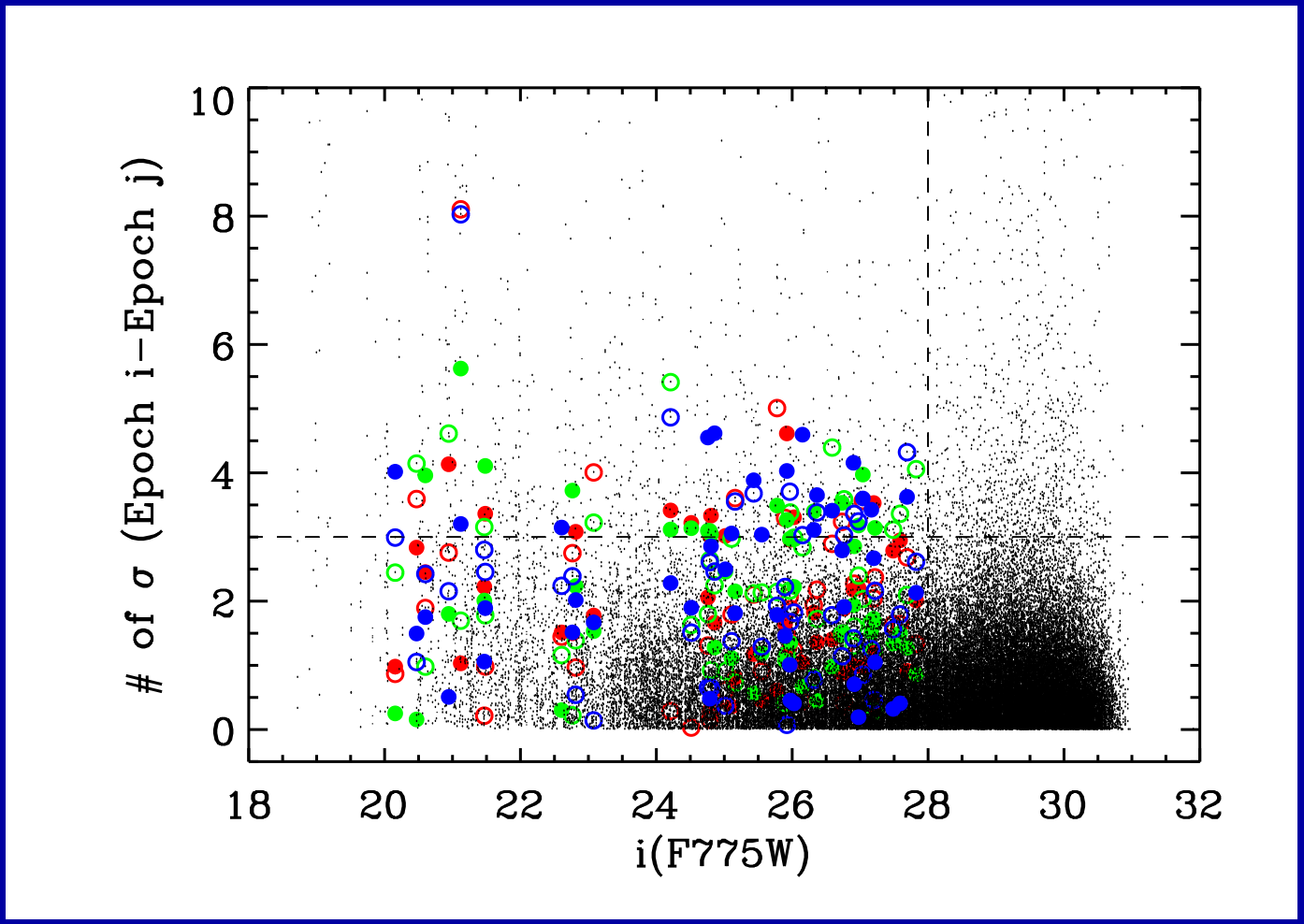

Main contamination are brighter objects over-deblended by object finder, *e.g.*, pieces of spiral arms — must weed these out visually.

- 6 out of 16 Chandra sources are faint point-like variable objects at $\gtrsim 3.0\sigma$. Other 10 Chandra sources are mostly brighter (early-type) galaxies, one is $\gtrsim 3.0\sigma$ variable $\Rightarrow$ Variable point sources are valid AGN candidates.
- We only sample ΔFlux $\gtrsim$10%—30% on timescales of months. The AGN sample is not complete — we miss all non-variable and the obscured AGN.

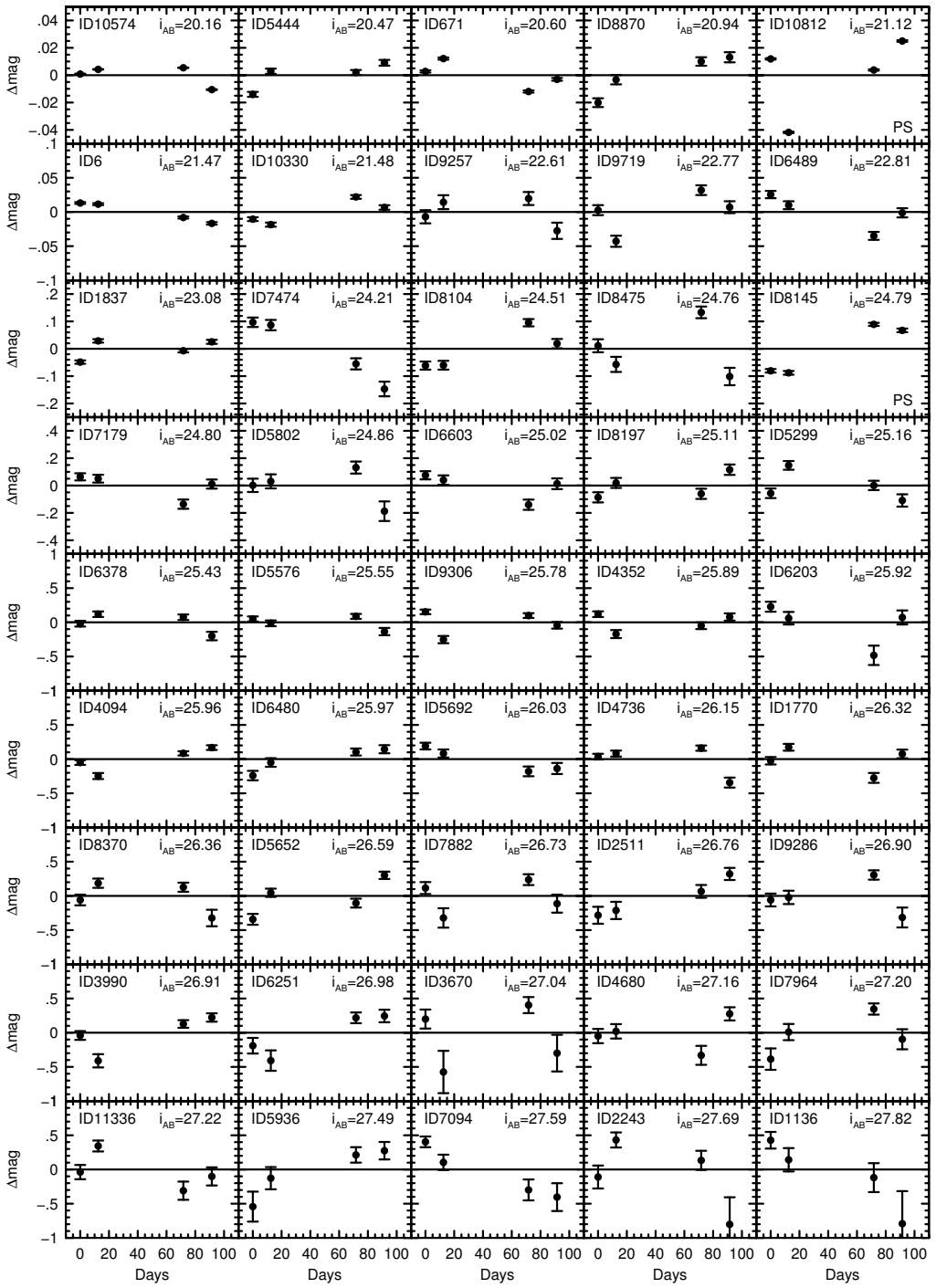

- Light curves: Can detect bright HUDF variables if $|\Delta\mathrm{mag}| \lesssim 1$–$2\%$!

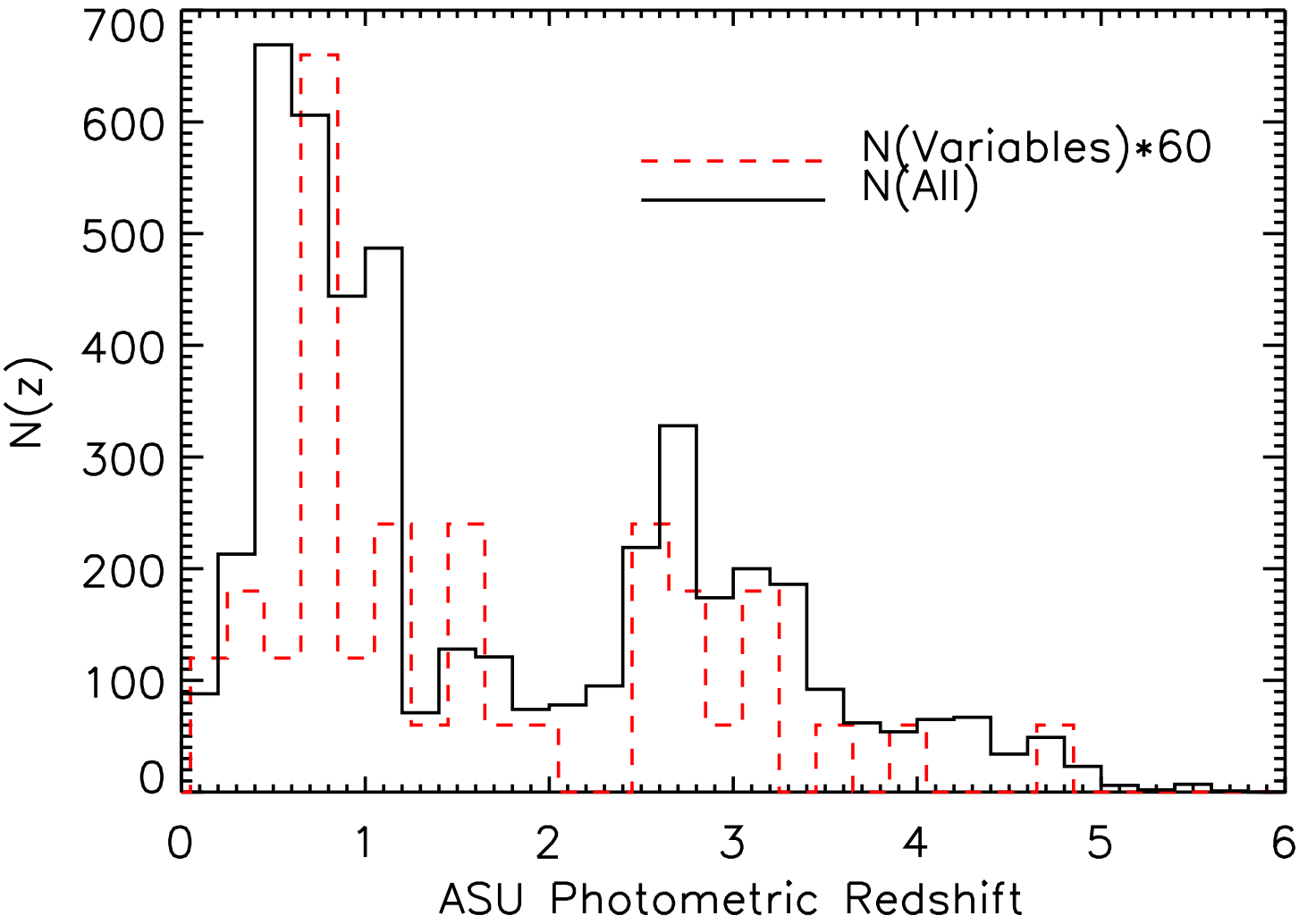

BViz(JH) Photo-z distribution of variable objects in the HUDF:

Full drawn: All HUDF field galaxies.

Dashed: HUDF variable objects ($\times 60$ for comparison with field galaxies).

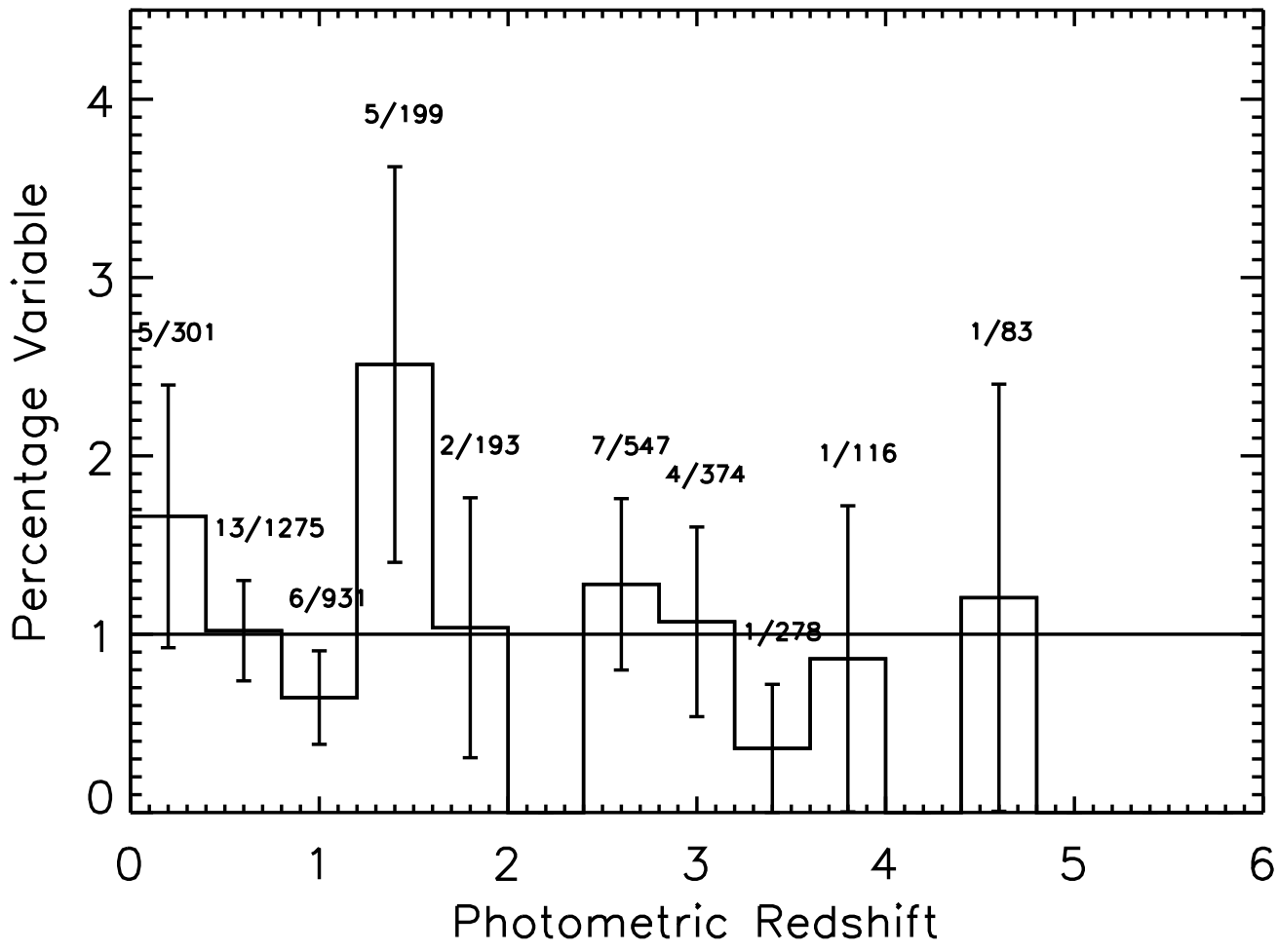

Fractional N(z) of HUDF variable objects compared to all HUDF galaxies.

- Variable objects show a similar N(z) as field galaxies. About 1% of all field galaxies have variable weak AGN at all redshifts.

$\Rightarrow$ If variable objects are representative of all weak AGN, SMBH growth keeps pace with the cosmic SFR (which peaks at $z \simeq 1$–2).

(3) A Study of Variable Objects in the HUDF

- HUDF variable fraction to AB$\lesssim$28.0 mag is $\sim$1% of all objects.

- These are likely a combination of weak AGN. None were SNe in distant galaxies (Strolger & Riess et al. 2004). None were novae and/or Long Period Variables in nearby galaxies (z$\lesssim$0.03).

- Accounting for limited time span, the real fraction of AGN in the HUDF that is variable on timescales of months is likely $\sim$2%, constraining the frequency of weak AGN activity and the fraction of hidden AGN.

- The variable-object N(z) follows that of all HUDF galaxies.

- At the median z$\simeq$1.5, objects are $\sim$3.6 Gyr old if born at z$\sim$7. If AGN life-time is several$\times 10^7$ years then $\lesssim$1–2% of all HUDF galaxies may be AGN. In AGN unification picture, $\sim$1/3 of these are seen as "face–on", consistent with the $\lesssim$1% HUDF variable AGN fraction ($when$ sampled on months time-scales; Psaltis et al. 2002).

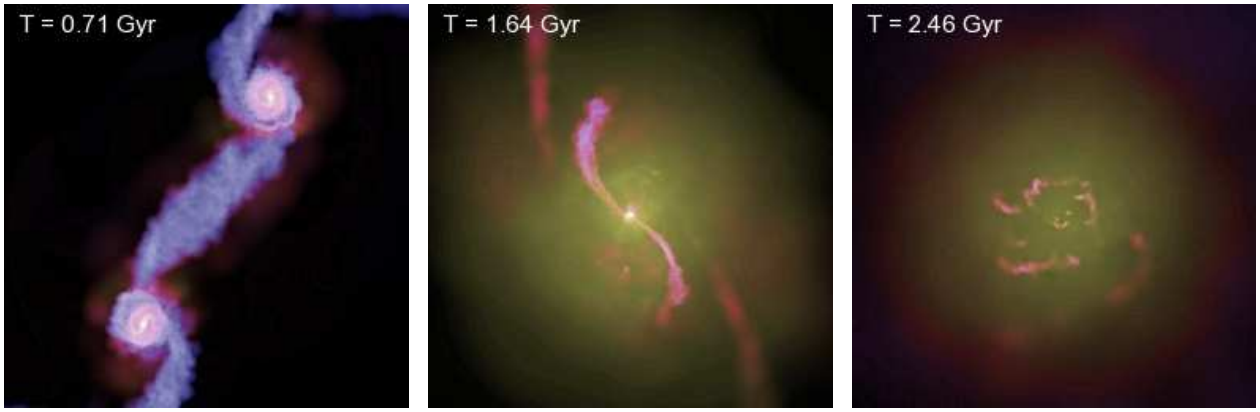

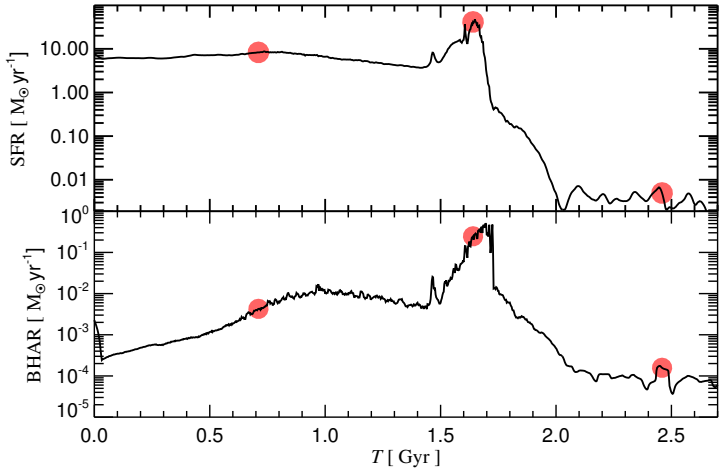

• [LEFT] Simulated merger of two disk galaxies at three different stages, including the effects of black hole growth and AGN feedback by Springel, di Matteo, Hernquist (2005, ApJ, 620, 79). The images show the gas distribution in the two disks at three different times, with color encoding temperature, while brightness measures gas density.

• [RIGHT] Evolution of the accretion rate onto the black holes (top) and the star formation rate (bottom). Red symbols mark the times shown in the three simulated images.

• Overlap between Tadpoles and Variables is very small — 1 object!
$\Leftrightarrow$ In hydrodynamical simulations, the object resembles a tadpole galaxy $\sim$0.7 Gyr after the merger starts, and the AGN is triggered $\gtrsim$1.6 Gyr after it starts, $i.e.$, $\gtrsim$1 Gyr after the tadpole stage.

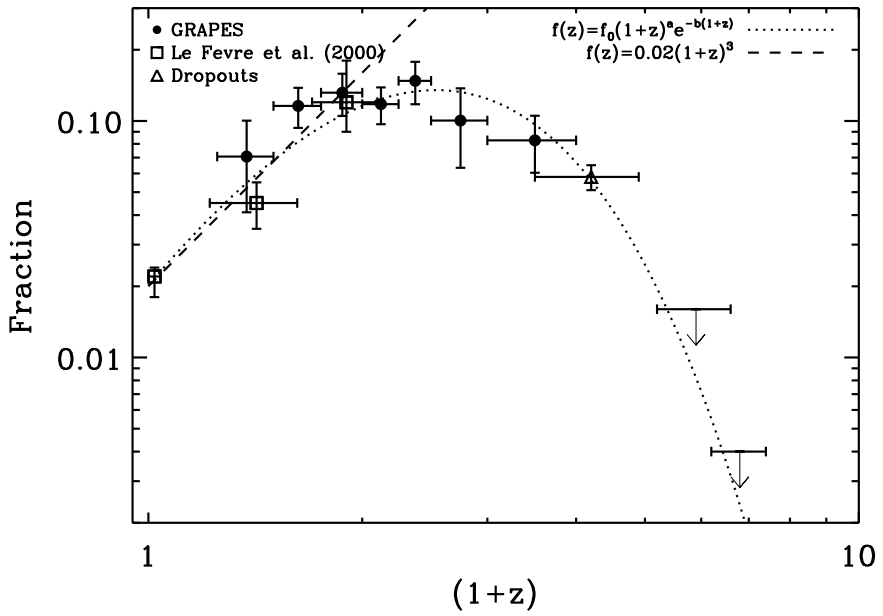

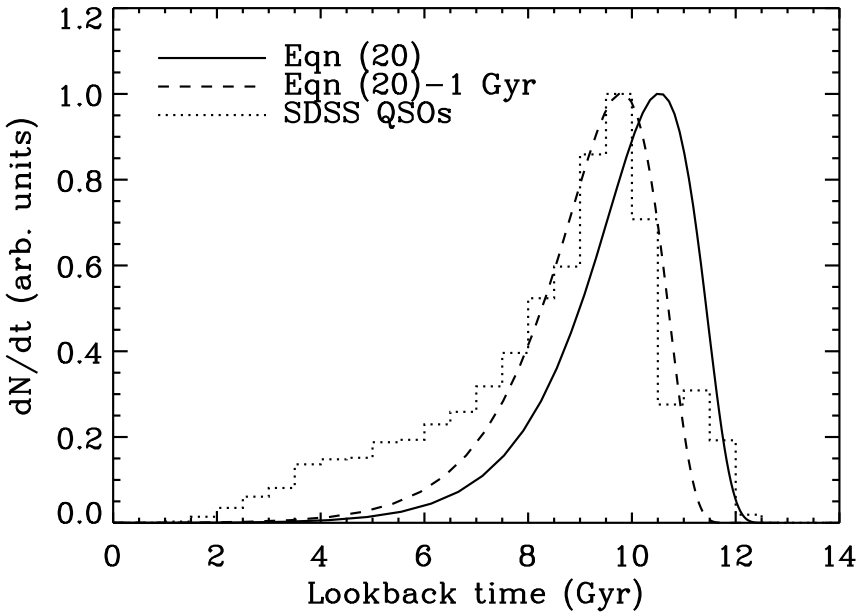

Ryan et al. (2007): Analytical model for epoch dependent merger rate, based on mean-free-path between galaxies in a ΛCDM universe — Follows the observed galaxy pair counts very well.

Galaxy merger rate compared to Sloan SDSS Quasar counts as function of look-back time — fairly similar curves except for $\sim$1 Gyr offset.

$\Rightarrow$ This qualitatively supports the presented picture — there may be a $\sim$1 Gyr delay between galaxy merger and SMBH feeding.

- The Beast feeds like fireflies in the night, and well after the Beauty produces its spectacular galaxy merging.

(4) Summary and Conclusions

- Tadpole galaxies make up about 6% of the total HUDF galaxy sample.
- Tadpoles have a redshift distribution very similar to that of field galaxies $\Longleftrightarrow$ Tadpole galaxies may be good tracers of the galaxy assembly process.
- Variable objects make up $\sim$1% of the total HUDF galaxy sample. Weak variable AGN comprise likely $\gtrsim$3–6% of total HUDF galaxy sample, when accounting for the missed long-period variable and obscured AGN.
- Variable objects have a redshift distribution similar to that of HUDF field galaxies $\Leftrightarrow$ They likely trace brief(!) episodes of SMBH growth.
- Both the HUDF Tadpoles and objects with Variable point sources have similar redshift distributions N(z), both of which peak around z$\simeq$1–2.

$\Rightarrow$ AGN GROWTH STAYS $\sim$IN PACE WITH GALAXY ASSEMBLY.

(5a) Future studies with the James Webb Space Telescope

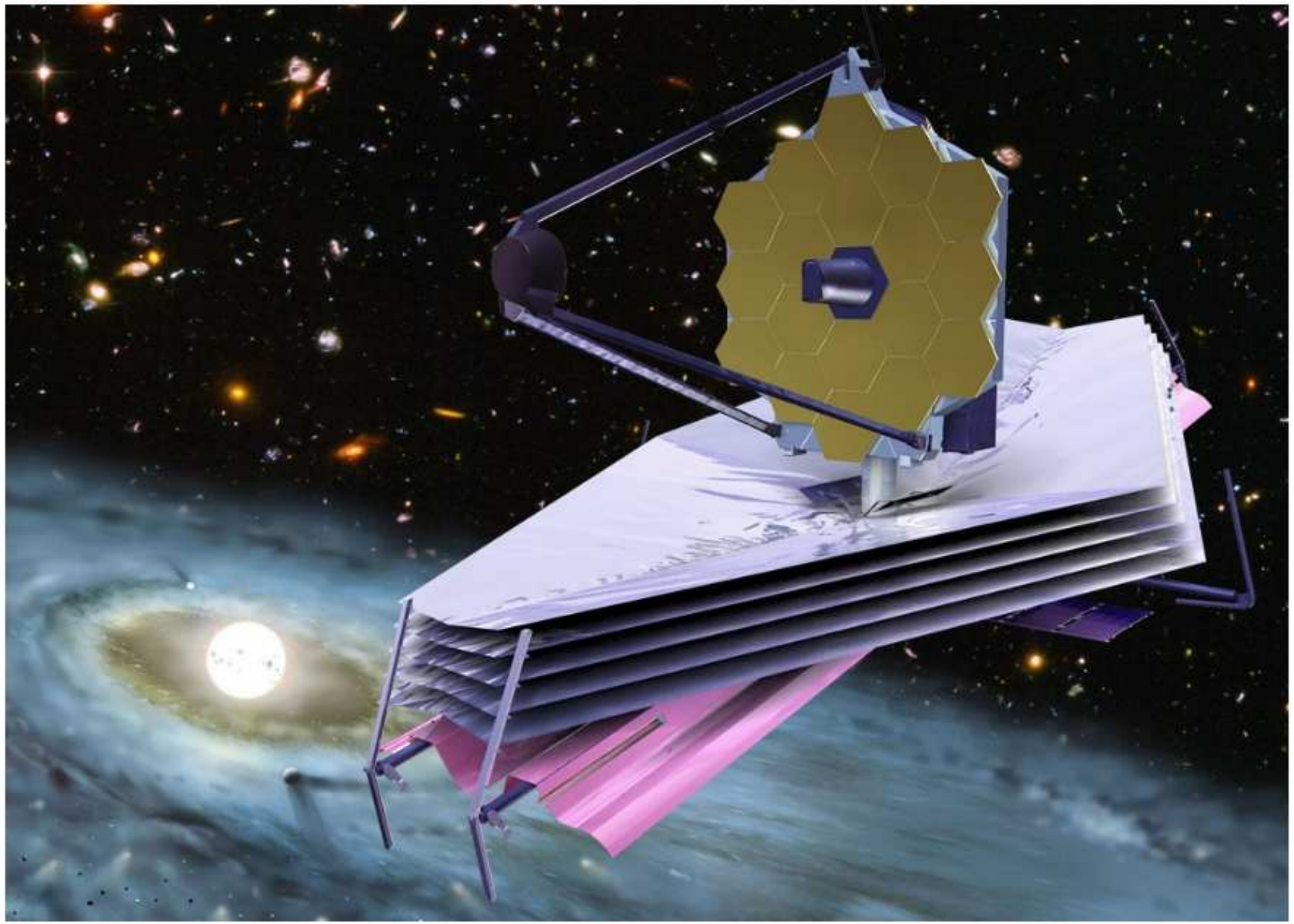

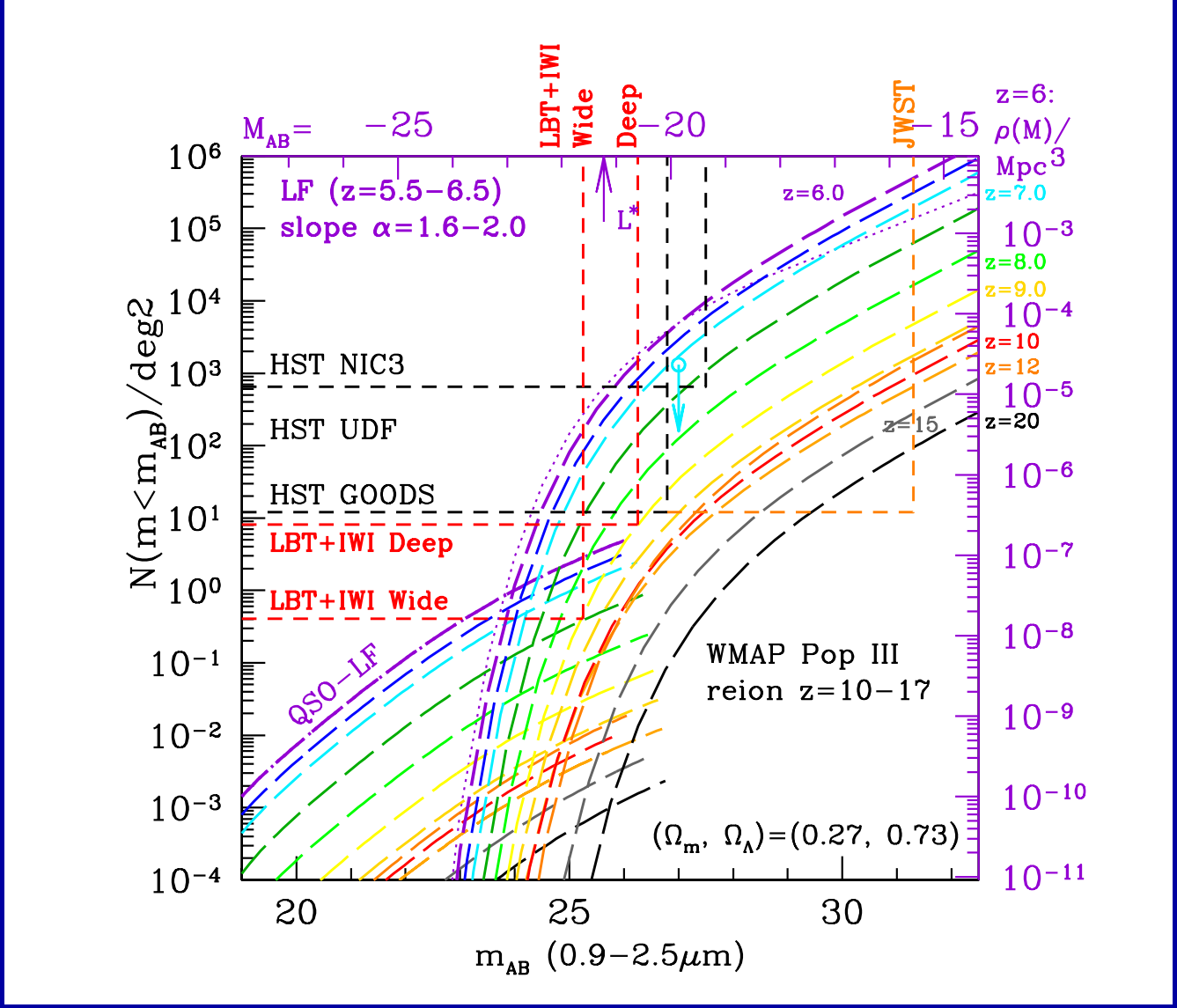

- Red boundaries indicate part of the galaxy and QSO LF that 4–10m class telescopes with wide-field IRCam can explore to $z=10$ and AB$\lesssim$25 mag.
- A ground-based wide-field near-IR survey to AB$\lesssim$25 mag $z\lesssim10$ is an essential complement to the JWST First Light studies:
- Co-evolution of supermassive black-holes and proto-bulges for $z\lesssim10$.

(5b) Future studies with the Hubble Wide Field Camera 3

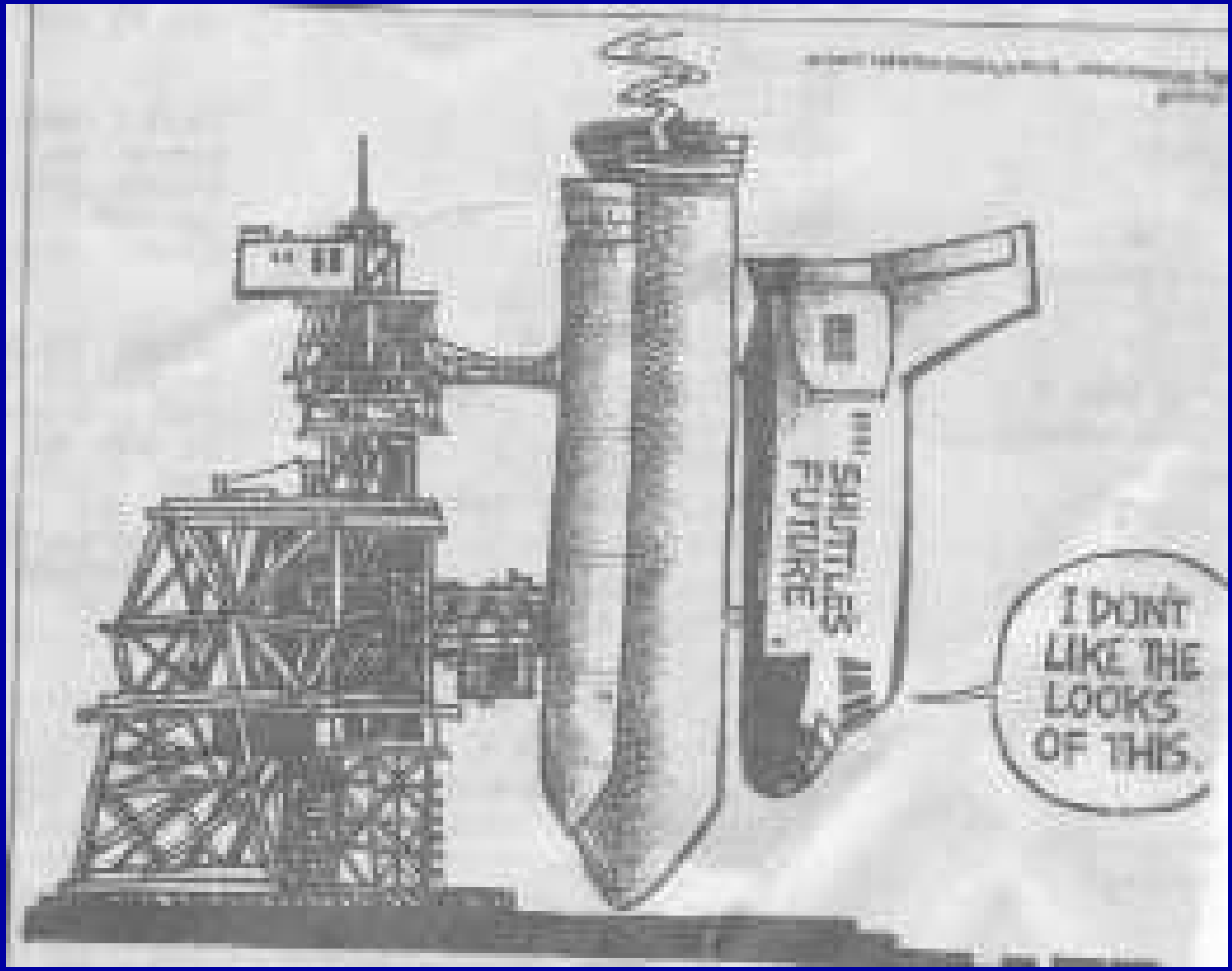

If there are no further Shuttle issues, WFC3 will get launched in Sep. 2008 ...

Power of combination of Grism and Broadband for WFC3

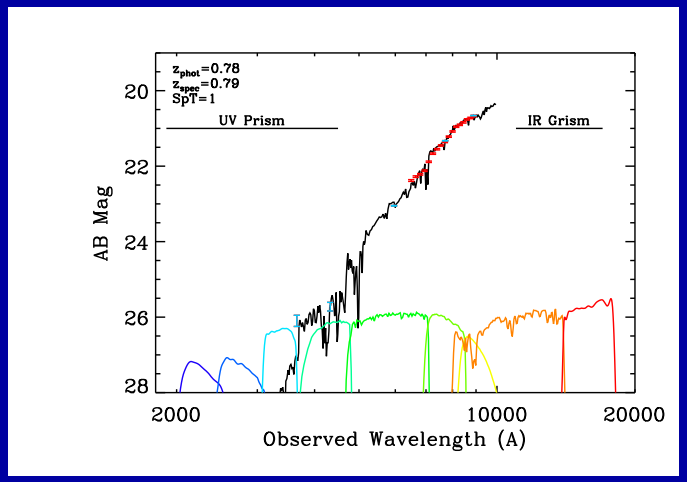

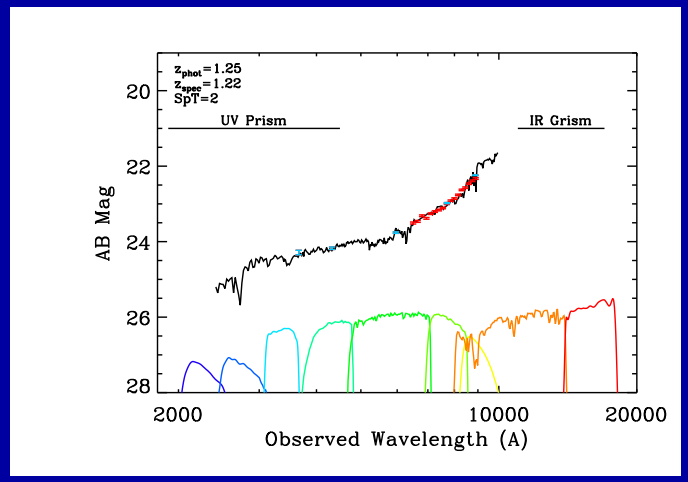

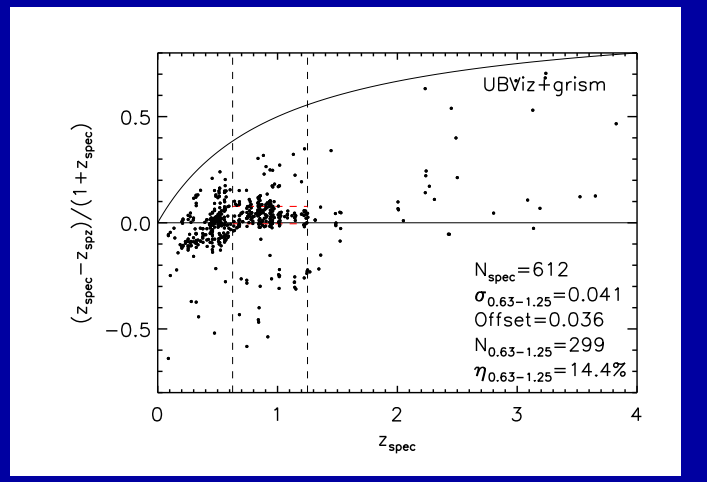

Lessons from the Hubble ACS grism surveys "GRAPES" and "PEARS" (Malhotra et al. 2005; Cohen et al. 2007; Ryan et al. 2007):

- (a) Spectro-photo-z's from HST grism + BViz(JH) considerably more accurate than photo-z's alone, with much smaller catastrophic failure %.
- (b) Redshifts for $\gtrsim$5000 objects to AB$\gtrsim$27.0–27.5 mag with $\sigma_z/(1+z)\lesssim 0.04$.
- (c) Expect $\lesssim$0.02–0.03 accuracy when including new capabilities of WFC3: UV and near-IR broad-band imaging and low-res grism spectroscopy.
- WFC3 will provide full panchromatic sampling of faint galaxy spectra from 0.2–1.7 μm, permitting high accuracy photo-z's for faint galaxies of all types to AB$\simeq$27.0 mag.

LF Faint-end Slope Evolution (fundamental, like local IMF)

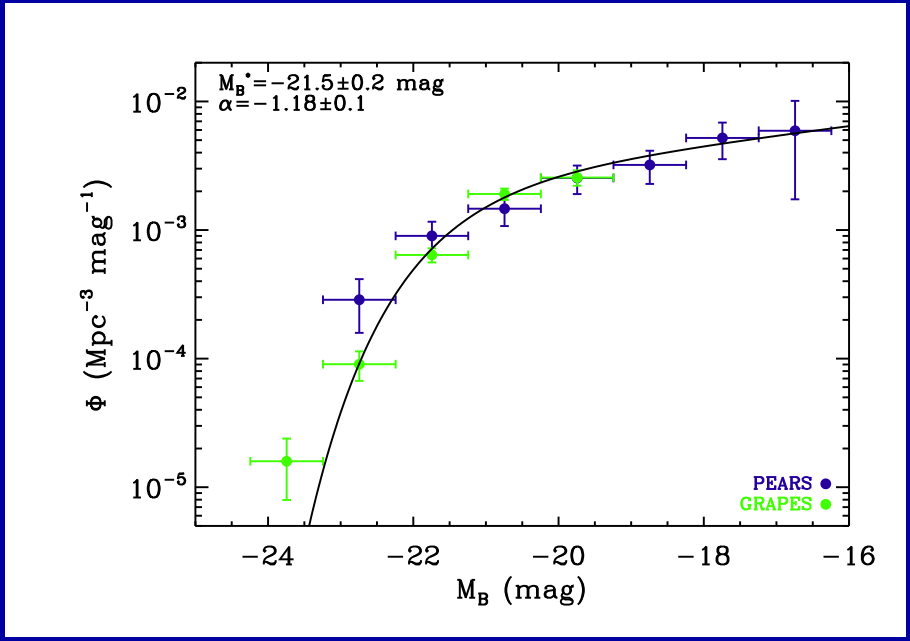

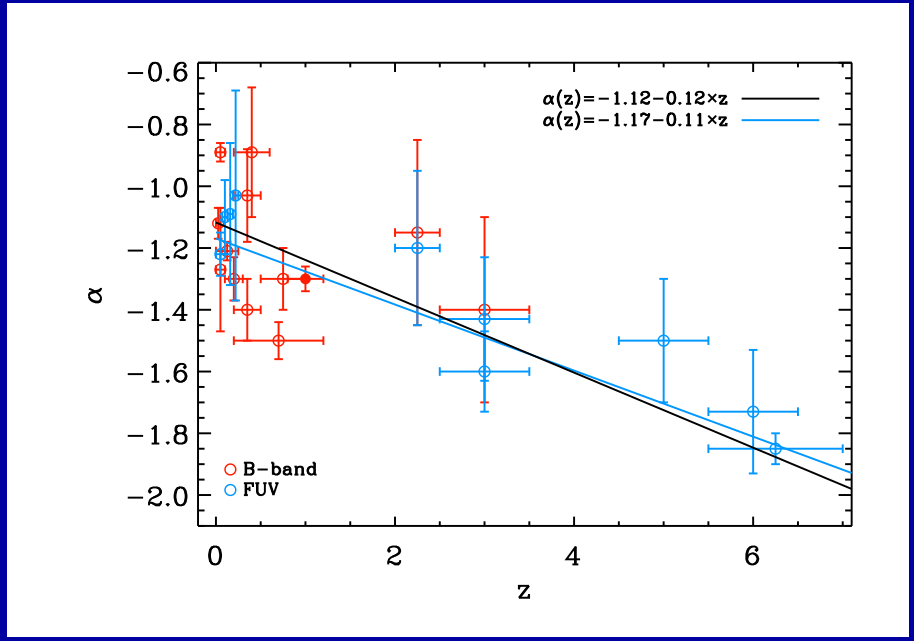

Measuring the faint-end of the LF at z$\simeq$0.7–3 with accurate z's to AB$\lesssim$27 mag is an extremely important constraint to hierarchical formation theories. WFC3 and JWST can do this deeper, and at lower spectral resolution than ground based spectroscopy (see PEARS survey, Ryan et al. 2007).

- WFC3 & JWST will fill data gap at 0.7$\lesssim$z$\lesssim$10 in different environments.
- Constraints to AGN and SF Feedback processes: these produce different faint-end slopes and slope-evolution, which WFC3 and JWST will measure.
- Measure environmental impact on LF faint-end slope directly: Significant (low-z) scatter is likely due to different clustering environments.